

University of Windsor

## Scholarship at UWindor

---

Electronic Theses and Dissertations

Theses, Dissertations, and Major Papers

---

7-4-2023

# Investigating Structural Determinants of the hYVH1-Hsp70 Interaction Using High Resolution Mass Spectrometry

Adrian A. Luiso  
*University of Windsor*

Follow this and additional works at: <https://scholar.uwindsor.ca/etd>

 Part of the [Biochemistry Commons](#)

---

### Recommended Citation

Luiso, Adrian A., "Investigating Structural Determinants of the hYVH1-Hsp70 Interaction Using High Resolution Mass Spectrometry" (2023). *Electronic Theses and Dissertations*. 9339.  
<https://scholar.uwindsor.ca/etd/9339>

This online database contains the full-text of PhD dissertations and Masters' theses of University of Windsor students from 1954 forward. These documents are made available for personal study and research purposes only, in accordance with the Canadian Copyright Act and the Creative Commons license—CC BY-NC-ND (Attribution, Non-Commercial, No Derivative Works). Under this license, works must always be attributed to the copyright holder (original author), cannot be used for any commercial purposes, and may not be altered. Any other use would require the permission of the copyright holder. Students may inquire about withdrawing their dissertation and/or thesis from this database. For additional inquiries, please contact the repository administrator via email ([scholarship@uwindsor.ca](mailto:scholarship@uwindsor.ca)) or by telephone at 519-253-3000ext. 3208.

**Investigating Structural Determinants of the hYVH1-Hsp70 Interaction  
Using High Resolution Mass Spectrometry**

By

**Adrian Luiso**

A Thesis  
Submitted to the Faculty of Graduate Studies  
through the Department of Chemistry and Biochemistry  
in Partial Fulfillment of the Requirements for  
the Degree of Master of Science  
at the University of Windsor

Windsor, Ontario, Canada

2023

© 2023 Adrian Luiso

**Investigating Structural Determinants of the hYVH1-Hsp70 Interaction Using High Resolution Mass Spectrometry**

by

**Adrian Luiso**

APPROVED BY:

---

A. Hubberstey  
Department of Biomedical Sciences

---

S. Pandey  
Department of Chemistry and Biochemistry

---

P.O. Vacratsis, Advisor  
Department of Chemistry and Biochemistry

June 9, 2023

## DECLARATION OF CO-AUTHORSHIP / PREVIOUS PUBLICATION

### I. Co-Authorship

I hereby declare that this thesis incorporates material that is result of joint research, as follows:

*Chapter 3 of this thesis includes the outcome of publications which have the following other co-authors: with DaDalt, AA, Bonham, CA, Lotze, GP, and Vacratsis, PO. In all cases only my primary contributions towards these publications are included in this thesis. The majority of the paper was produced with research by Dadalt, AA, and Bonham, CA, with experiments by Lotze, GP also performed in response to reviewer commentary. Data analysis and experimental design was provided by Vacratsis, PO.*

I am aware of the University of Windsor Senate Policy on Authorship and I certify that I have properly acknowledged the contribution of other researchers to my thesis, and have obtained written permission from each of the co-author(s) to include the above material(s) in my thesis.

I certify that, with the above qualification, this thesis, and the research to which it refers, is the product of my own work.

### II. Previous Publication

This thesis includes [1] original papers that have been previously published/submitted to journals for publication, as follows:

Thesis Chapter	Publication title/full citation	Publication status*

<i>Chapter 3</i>	<i>DaDalt AA, Bonham CA, Lotze GP, Luiso AA, Vacratsis PO. Src-mediated phosphorylation of the ribosome biogenesis factor hYVH1 affects its localization, promoting partitioning to the 60S ribosomal subunit. J Biol Chem. 2022 Dec;298(12):102679.</i>	<i>Published</i>
------------------	--	------------------

I certify that I have obtained a written permission from the copyright owner(s) to include the above published material(s) in my thesis. I certify that the above material describes work completed during my registration as a graduate student at the University of Windsor.

### III. General

I declare that, to the best of my knowledge, my thesis does not infringe upon anyone's copyright nor violate any proprietary rights and that any ideas, techniques, quotations, or any other material from the work of other people included in my thesis, published or otherwise, are fully acknowledged in accordance with the standard referencing practices. Furthermore, to the extent that I have included copyrighted material that surpasses the bounds of fair dealing within the meaning of the Canada Copyright Act, I certify that I have obtained a written permission from the copyright owner(s) to include such material(s) in my thesis.

I declare that this is a true copy of my thesis, including any final revisions, as approved by my thesis committee and the Graduate Studies office, and that this thesis has not been submitted for a higher degree to any other University or Institution.

## ABSTRACT

The protein tyrosine phosphatase hYVH1 (also known as DUSP12) is an atypical member of the DUSP subfamily of PTPs that possesses a unique C-terminal zinc-binding domain and demonstrates functions in cell survival, cell cycle regulation, stress granule disassembly, and ribosome biogenesis. hYVH1 has been shown to associate with the ATPase domain of Hsp70 to amplify its cell survival capability, and recent studies have suggested that this complex can be dissociated by Src kinase phosphorylation. This study demonstrates the relevancy of Src-mediated hYVH1 phosphorylation at the endogenous level, supporting the conclusion that hYVH1 is a novel Src substrate. Label-free quantitative mass spectrometry confirmed a 29% decrease in Hsp70 co-immunoprecipitation in response to Src expression. Orthogonal structural mass spectrometry approaches were used to propose a binding interface on hYVH1 for the interaction with Hsp70, with results from limited proteolysis and differential biotin labelling indicating a peptide region between residues 50-77 on the extreme portion of the N-terminal catalytic domain. Phosphosite mapping of hYVH1 was undertaken to elucidate a mechanism by which Src may abrogate the complex, with targeted mass spectrometry methods helping to identify Tyr35 on hYVH1 as a novel Src phosphorylation site. Upon mutation of Tyr35 to a Glu residue, the hYVH1-Hsp70 complex displayed increased association, suggesting that Src phosphorylation of Tyr35 is not the regulatory mechanism for hYVH1-Hsp70 complex attenuation. These results imply that phosphorylation of Hsp70, not hYVH1, may drive dissociation, although hYVH1 may be required to recruit Src to the complex.

## **DEDICATION**

*To my girlfriend Brittany*

## ACKNOWLEDGEMENTS

The past two and a half years of study at the University of Windsor have simultaneously felt like the most valuable learning experience of my life and the most fun I will probably ever have at school. Although the near entirety of this document is a testament to the former, I would like to take a couple of pages to focus on the latter.

First and foremost, I would like to express a huge thank you to my supervisor, Dr. Otis Vacratsis, for granting me the privilege to learn in his lab and for investing in my development as a student. If not for the hours he spent helping me with data processing, his availability to my constant questions, and his general commitment to his students, this thesis would not make it across the finish line. You are a superstar, OV! Similarly, I would like to express gratitude to my committee, Dr. Siyaram Pandey and Dr. Andrew Hubberstey, for their willingness to take time out of their busy schedules and oversee my project and provide feedback. Also, to the professors at this school with whom I have had the pleasure to GA for: Dr. Kenneth Ng, Dr. Sirinart Ananvoranich, Dr. Drew Marquardt, Dr. Anna Kozarova, and Dr. Zareen Amtul – if I ever find future success as a teacher, I owe it in large part to the example set by these professors at UWindsor.

Truly, the real master's degree was the friends we made along the way. I want to extend my thanks to Dr. Ashley DaDalt and Cody Caba, as well as Dr. Justin Roberto for all the help and training they provided over the years, and for making sure that I never choked on crayons in the HQP. I would also like to extend

a thank you to my fellow graduate students – Kaitlyn Hand, Lucas Campo, Fasih Rehman, Jessica Szawara, and Lucas Vajko-Siddall; as well as the undergraduates that I had the pleasure of working with – Alex Colak, Lauren Pupulin, Lithmi Jayasinghe, Grace Querbach, and Steven Tambakis. I would like to give special acknowledgements to Patrick Blendea, and Nick Rowland (school isn't the same without you buddy). Without all of you, this experience would not be nearly as enjoyable. Lastly, I want to acknowledge Griffin Lotze, who has been my lab partner since Grade 11 chemistry, and is currently waiting for me to join him in graduating with an M.Sc. I value how we elevate each other to new heights and could not have asked for a better colleague and friend.

And, of course, none of this is possible without the support of my Mom, Dad, and my sister Erica, who celebrated my successes with me and helped me stay motivated during times of turbulence. We are the products of the family that raised us, and I have the good fortune of being raised by the best. This also extends to my aunts, uncles, cousins, and close friends I have struggled to keep in touch with – we will see each other soon. To my grandparents, Nonno Michele, Nonna Chiara, Nonna Filomena, and the late Nonno Benedetto, I hope I have made you all proud – *Ti voglio bene assai*.

Last and most certainly not least, I want to dedicate these past two and a half years of study to my girlfriend Brittany, who was always there to provide unconditional love and support and to inspire me to reach beyond my limits. You have the patience of a saint, and I am the luckiest man alive with you by my side. I love you Britt, and you mean the world to me.

## TABLE OF CONTENTS

<b>DECLARATION OF CO-AUTHORSHIP / PREVIOUS PUBLICATION</b> .....	iii
<b>ABSTRACT</b> .....	v
<b>DEDICATION</b> .....	vi
<b>ACKNOWLEDGEMENTS</b> .....	vii
<b>LIST OF FIGURES</b> .....	xi
<b>LIST OF ABBREVIATIONS</b> .....	xvi
<b>CHAPTER 1: INTRODUCTION</b> .....	1
<b><i>1.1 Mass Spectrometry in Proteomics</i></b> .....	<b>1</b>
<b><i>1.1.1 Tandem Mass Spectrometry (MS/MS)</i></b> .....	<b>3</b>
<b><i>1.2 Reversible Protein Phosphorylation Dynamics</i></b> .....	<b>7</b>
<b><i>1.3 Tyrosine Phosphatases and the PTP Superfamily</i></b> .....	<b>9</b>
<b><i>1.4 The Yeast Phosphatase: YVH1</i></b> .....	<b>12</b>
<b><i>1.5 The Human Phosphatase: hYVH1</i></b> .....	<b>13</b>
<b><i>1.6 hYVH1 in Cell Survival</i></b> .....	<b>17</b>
<b><i>1.7 Hsp70 and the association to hYVH1</i></b> .....	<b>18</b>
<b><i>1.8 Src Kinase and hYVH1</i></b> .....	<b>20</b>
<b><i>1.9 Ribosome Biogenesis and hYVH1</i></b> .....	<b>21</b>
<b><i>1.9.1 hYVH1 and Src at the 80S ribosome</i></b> .....	<b>22</b>
<b><i>1.10 Objectives</i></b> .....	<b>24</b>
<b>CHAPTER 2:</b>	
<b>MATERIALS AND METHODS</b> .....	<b>25</b>
<b><i>2.1 Plasmids</i></b> .....	<b>25</b>
<b><i>2.2 Cell Culture</i></b> .....	<b>25</b>
<b><i>2.3 Affinity Chromatography</i></b> .....	<b>27</b>
<b><i>2.4 Mass Spectrometry Sample Preparation and Analysis</i></b> .....	<b>28</b>
<b><i>2.4.1 NHS-Biotin Labelling and Limited Proteolysis</i></b> .....	<b>29</b>
<b><i>2.4.2 hYVH1 Phosphosite Mapping</i></b> .....	<b>30</b>

<b>2.5 SDS-PAGE and Western Blotting</b> .....	<b>32</b>
<b>CHAPTER 3:</b>	
<b>RESULTS AND DISCUSSION</b> .....	<b>34</b>
<b>3.1 Endogenous Phosphorylation of hYVHI by Src</b> .....	<b>34</b>
3.1.1 Rationale for Examining Endogenous Phosphorylation .....	34
3.1.2 Src Kinase Phosphorylates hYVHI .....	34
3.1.3 Endogenous Phosphorylation of hYVHI by Src.....	37
<b>3.2 Quantifying the hYVHI-Hsp70 Complex Dissociation by Src</b> .....	<b>40</b>
<b>3.3 The hYVHI-Hsp70 binding interface</b> .....	<b>42</b>
3.3.1 Rationale for Binding Site Identification .....	42
3.3.2 In-Solution Limited Proteolysis .....	42
3.3.3 NHS-biotin Labelling to Determine Binding Interface .....	46
3.3.4 N-terminal coIP of hYVHI .....	52
<b>3.4 Phosphosite Mapping of hYVHI</b> .....	<b>55</b>
3.4.1 Validating the Presence of Alternative Sites .....	55
3.4.2 SRM Mass Spectrometry with Ion Mobility .....	58
3.4.3 Characterization of Y35E Phosphorylation .....	61
<b>3.5 Proposed Model</b> .....	<b>66</b>
<b>CHAPTER 4:</b>	
<b>CONCLUSION AND FUTURE WORK</b> .....	<b>68</b>
<b>4.1 Conclusions</b> .....	<b>68</b>
<b>4.2 Future Work</b> .....	<b>69</b>
<b>REFERENCES</b> .....	<b>71</b>
<b>APPENDICES</b> .....	<b>77</b>
<b>Appendix A</b> .....	<b>77</b>
<b>VITA AUCTORIS</b> .....	<b>78</b>

## LIST OF FIGURES

**Figure 1.1 Schematic of vital components in a mass spectrometer.** **A)** A demonstration of electrospray ionization (ESI), outlining the droplet shrinking, and Coulombic explosion that results in analyte molecules abstracting protons from the acidic solvent. **B)** A quadrupole acting as a mass filter, only allowing molecules of a specific  $m/z$  to pass through and diverting non-resonant molecules away from detection. **C)** A collision cell, outlining the fragmentation of precursor analyte molecules by collision with helium. **D)** A time-of-flight tube (TOF), demonstrating the acceleration of fragment ions by the ion pusher, into a field-free region that is under vacuum. All fragments are given the same kinetic energy, but the smallest molecules with the highest charge will move fastest. The ion path is outlined by the dotted line. **E)** A sample MS/MS spectrum, with ion  $m/z$  plotted on the x-axis and ion abundance plotted on the y-axis.....**6**

**Figure 1.2 Protein Phosphorylation and Dephosphorylation.** The synergistic relationship of kinases and phosphatases. Kinases catalyze the transfer of a phosphate group from ATP to a free -OH group on an enzyme, producing ADP in the process. Phosphatases may then hydrolyze the phosphate to remove it from the enzyme, producing inorganic phosphate.....**8**

**Figure 1.3. The Cys-based PTP superfamily.** A phylogenetic tree displaying the relationship of Cys-based PTPs. Class II and III PTPs constitute 3 families, with a collective 5 enzymes between them. Class I PTPs possess several subclassifications, the largest of which are the classical “Receptor-like” and “Non-receptor-like” PTP subfamilies and the VH1-like or “DUSP” subfamily. The DUSPs are further subdivided into the MAP kinase phosphatases, Slingshots, Phosphatases of the regenerating liver, Cell Division Cycle 14, PTEN-like, myotubularin, and atypical DUSP subfamilies. Adapted from Tautz et al.....**10**

**Figure 1.4. The PTP catalytic mechanism.** The 2-step mechanism by which all Cys-based PTPs operate. The first step (pictured left) involves the nucleophilic attack of the P atom by the catalytic Cys, followed by hydrolysis of the phosphodiester bond by an Asp to release the substrate. The second step (pictured right) shows the regeneration of the enzyme via abstraction of a proton from the ordered water molecule by the Asp, and subsequent hydrolysis of the thiophosphate intermediate. Figure obtained from Tautz et al. ....**11**

**Figure 1.5. Sequence alignment of hYVH1 and YVH1 orthologues.** A sequence alignment of hYVH1 and orthologues, adapted from Muda et al.<sup>1</sup> N-terminal catalytic domain is outlined in red, C-terminal ZBD is outlined in green. Conserved Cys and His residues are highlighted in yellow. The active site Cys is highlighted in red. General amino acid conservation and functional conservation are outlined in respective colours. ....**14**

**Figure 1.6. The domain structure of hYVH1.** A predictive model of hYVH1 assembled through SwissMODEL by integrating X-ray crystallography data for the N-terminal DUSP domain (red), with a CryoEM structure for the ZBD (blue). The structure was formatted in PyMOL.....**16**

**Figure 1.7. Domain Structure of Hsp70.** X-ray crystallography structure of Hsp70, displaying N-terminal ATPase domain (red) and C-terminal Substrate-binding domain (blue), separated by a short linker region. The C-terminal domain is further subdivided, highlighting the helical lid subdomain (yellow) that folds over a substrate binding pocket. The structure was formatted in PyMOL. ....**18**

**Figure 3.1. Phosphorylation of hYVH1 by Src in both an overexpressed and endogenous model.** **A)** A demonstration of hYVH1 phosphorylation by Src using HeLa samples overexpressing FLAG-hYVH1, or FLAG-hYVH1 and Myc-Src. The two lanes on the right have been treated with alkaline phosphatase. The top panel shows Tyr phosphorylation on a FLAG-IP, the middle panel shows the presence of Src in the cellular lysates, and the bottom panel verifies the amount of FLAG-hYVH1 in each lane. **B)** ImageJ-obtained densitometry measurements of 4G10 blots for the two Src-transfected lanes. Normalized to the amount of FLAG-hYVH1 and Myc-Src present in each sample (n=5). **C)** Endogenous hYVH1 phosphorylation by Src in HeLa cells. The left lane is a rabbit serum control for the anti-hYVH1 IP. The centre lane is treated with DMSO, and the right lane is treated with SI-1. The top panel is a blot for tyrosine phosphorylation of an hYVH1-IP, and the bottom panel is a blot for hYVH1 in an hYVH1-IP. **D)** ImageJ-obtained densitometry measurements of 4G10 blots for the two experimental lanes. Normalized to the amount of hYVH1 present in each sample (n=4). .....**36**

**Figure 3.2. Workflow for determining the endogenous phosphorylation of hYVH1 by Src kinase.** HeLa cells were serum starved for 24 hours, then incubated with fresh FBS and pervanadate to stimulate tyrosine phosphorylation by Src and inhibit PTP activity. Plates were administered either the SI-1 Src inhibitor, or DMSO at this time. After 40 minutes, they were treated with EGF for 20 minutes to trigger growth-factor induced Src activation, then lysed and immunoprecipitated with a rabbit anti-hYVH1 antibody that was prebound to a Protein A agarose resin. Figure produced in BioRender. ....**38**

**Figure 3.3. Quantitation of Src's effect on hYVH1's ability to coIP Hsp70.** A bar graph of aggregated MS data, highlighting the difference in Hsp70 coIP efficiency in the presence of Src. All hYVH1 and Hsp70 peptides were normalized to the top three most abundant peptides in each sample, and then normalized to the amount of hYVH1 between all trials and samples (n=3). All trials were then normalized to the -Src sample, and the averages are expressed. ....**41**

**Figure 3.4. Results of the limited digest of hYVH1.** **A)** A bar graph displaying the significant differentially encountered peptides (n=3), relative to a control peptide that remained unchanged in abundance between samples after normalization. The identified peptides were all considered for normalization to acquire a correction factor to apply using the Progenesis software. Peptides reproducibly above a 1.5-fold change were considered significant. **B)** The amino acid sequence of hYVH1, illustrating the peptides identified by limited digestion in red and blue (coloured to show peptide boundaries). Sequence coverage is expressed as a percentage at the bottom. **C)** Tables showing significant peptides identified from all three trials of limited in-solution trypsin proteolysis. The peptide corresponding to amino acids 50-67 is highlighted in red.

..... 44-45

**Figure 3.5. Workflow to determine the binding interface via NHS-biotinylation.** Transfected samples were lysed and then subjected to anti-FLAG IP. NHS-biotin was added to the washed resin and incubated for 30 minutes, followed by washing in glycine. These samples were then digested in solution with trypsin, subjected to thiol reduction and alkylation, and desalted with an Oasis column before MS analysis. Figure produced in BioRender.....47

**Figure 3.6 MS spectra of biotinylated peptides.** **A)** Representative mass spectra of NHS-biotin treated samples from HeLa cells transfected with His-Hsp70 and FLAG-hYVH1 (top) and transfected with FLAG-hYVH1 and Myc-Src (bottom). **B)** A bar graph displaying the significant biotinylated peptide corresponding to amino acids 50-77, relative to a control peptide that remained unchanged in abundance between samples. All biotin-containing peptides were considered for normalization to acquire a correction factor to apply using the Progenesis software. Peptides reproducibly above a 1.5-fold change were considered significant. (n=3) **C)** Tables showing significant peptides identified from all three trials of the NHS-biotin labelling experiment. The peptide corresponding to amino acids 50-77 is highlighted in red, the control peptide selected is highlighted in blue.

..... 49-50

**Figure 3.7 The proposed N-terminal binding region on hYVH1.** **A)** The predicted structure of hYVH1 with the proposed Hsp70-binding region highlighted in green, with side chains visible. Structure produced in PyMOL. **B)** A zoomed-in view of the binding site structure, with Asp74, Glu73, Lys67, and Ser65 highlighted. Image produced from the hYVH1 N-terminal crystal structure on the Protein Data Bank (Accession: 4JNB).....52

**Figure 3.8. N-terminal coIP of Hsp70 by hYVH1.** **A)** HeLa cells transfected with the indicated samples were lysed and subjected to a FLAG IP. From left to right: empty vector (EV), Hsp70, Hsp70 + hYVH1(WT), Hsp70 + hYVH1 ΔZBD, Hsp70 + hYVH1 ΔZBD + Src, Hsp70 + Src, hYVH1 ΔZBD + Src, hYVH1

$\Delta$ ZBD, and Src. The 5 panels shown are in descending mass order (kDa; shown on the left) and depict (from top to bottom): anti-His on a FLAG-IP, anti-His + anti-Src on lysates, anti-FLAG on a FLAG-IP, anti-4G10 on a FLAG-IP, and anti-FLAG on a FLAG-IP. hYVH1 is FLAG-tagged whereas Hsp70 is His<sub>6</sub>-tagged. **B)** ImageJ-obtained densitometry measurements of anti-His blots for the 4<sup>th</sup> and 5<sup>th</sup> lanes (sample ID on x-axis). Normalized to the amount of FLAG-hYVH1 present in the FLAG-IP and His-Hsp70 present in the lysates (n=3). .....53

**Figure 3.9. Src Phosphorylation of hYVH1 Y179F.** **A)** A Western blot showing the phosphorylation of hYVH1 Y179F by Src following FLAG IP from HeLa cells. Samples are overexpressing FLAG-hYVH1 Y179F, or FLAG-hYVH1 Y179F and Myc-Src. The two lanes on the left have not been treated with alkaline phosphatase, and the two lanes on the right have. All four lanes have been treated with sodium orthovanadate. The top panel shows Tyr phosphorylation on a FLAG-IP, the middle panel shows the presence of Src in the cellular lysates, and the bottom panel verifies the amount of FLAG-hYVH1 in each lane. **B)** ImageJ-obtained densitometry measurements of 4G10 blots for the two Src-transfected lanes. Normalized to the amount of FLAG-hYVH1 and Myc-Src present in each sample (n=3). .....56

**Figure 3.10 Potential phosphotyrosine sites on hYVH1.** The 3D structure of hYVH1 with all Tyr residues in yellow, and Tyr179 in green. These are highlighted and numbered on the amino acid sequence below, which is coloured in alternating red and blue to delineate the boundaries of possible tryptic peptides (excluding the probable missed cleavages). Structure produced in PyMOL..... 57

**Figure 3.11 Workflow for hYVH1 phosphosite mapping.** HeLa cells in culture were transfected with either hYVH1 + EV or hYVH1 + Src, then treated with sodium pervanadate for 1 hour before lysis. FLAG-IP was performed to isolate hYVH1, followed by an on-bead digestion with trypsin. Samples were then reduced and alkylated with DTT and IAA, before cleanup with an Oasis column and subsequent MS analysis. Figure produced in BioRender.....58

**Figure 3.12 MS fingerprint for phosphosite mapping.** An MS “fingerprint” spectrum that outlines the abundances of precursor peptide ions for both the hYVH1 + EV sample (top) and the hYVH1 + Src sample (bottom)......59

**Figure 3.13. MS/MS of a putative phosphorylation site.** An MS/MS spectrum produced from the fragmentation of the tryptic peptide located between amino acid positions 21-49, resolved using SRM techniques. The precursor ion is indicated by the arrow, with the sequence above showing the positions of the y and b ions. y and b ions are indicated on the spectrum above their respective peaks.....60

**Figure 3.14. The Tyr35 phosphorylation site architecture and conservation.** **A)** The location of Tyr35 and nearby polar residues in the X-ray crystallography structure; provided by the Protein Data Bank (Accession: 4JNB). **B)** A sequence alignment between *H. sapiens*, *M. musculus*, *S. cerevisiae*, and *S. pombe*,

displaying residues 1-39; produced in ESPript, using alignment generated by T-Coffee.....**62**

**Figure 3.15. MS results from hYVH1 Y35E and Hsp70 coIP.** A graph displaying the difference in Hsp70 coimmunoprecipitation between wild-type (WT) hYVH1 (blue) and hYVH1 Y35E (green) from HeLa cells. All hYVH1 and Hsp70 peptides were normalized to the top three most abundant peptides in each sample, and then normalized to the amount of hYVH1 between all trials and samples (n=3). All trials were then normalized to the WT sample, and the averages are expressed.....**63**

## LIST OF ABBREVIATIONS

- AB – ammonium bicarbonate
- ACN – acetonitrile
- ADP – adenosine diphosphate
- ATP – adenosine triphosphate
- BSA – bovine serum albumin
- CID – collision-induced dissociation
- CIP – calf intestinal phosphatase
- Cys/C – cysteine
- DC – direct current
- DDA – data-dependent acquisition
- DIA – data-independent acquisition
- DMEM – Dulbecco's Modified Eagle's Medium
- DMSO – dimethyl sulfoxide
- DNA – deoxyribonucleic acid
- DTT – dithiothreitol
- DUSP/DSP – dual-specificity phosphatase
- EF2 – elongation factor 2
- EGF – epidermal growth factor
- EIF6 – eukaryotic initiation factor 6
- ESI – electrospray ionization
- EV – empty vector
- FA – formic acid
- FBS – fetal bovine serum

FMRP – fragile-X mental retardation protein

HeLa – Henrietta Lacks

Hsp70 – 70kDa heat shock protein

hYVH1 – human yeast vaccinia homolog 1

IAA – iodoacetamide

IP – immunoprecipitation

Lys/K – lysine

m/z – mass to charge ratio

MALDI – matrix-assisted laser desorption/ionization

MKP – mitogen activated protein kinase phosphatase

mRNA – messenger ribonucleic acid

Mrt4 – mRNA turnover 4

MS – mass spectrometry

PBS – phosphate-buffered saline

PCR – polymerase chain reaction

PDGF – platelet-derived growth factor

PEI – polyethylenimide

PRL – protein of the regenerating liver

PSP – protein serine/threonine phosphatase

PTEN – phosphatase and tensin homolog

PTM – post-translational modification

PTP – protein tyrosine phosphatase

pTyr – phosphotyrosine

PVDF – polyvinylidene fluoride

RACK1 – receptor for activated C kinase 1

RF – radio frequency  
RNP – ribonucleoprotein  
RPLC – reverse-phase liquid chromatography  
rRNA – ribosomal ribonucleic acid  
SDS – sodium dodecyl sulfate  
Ser/S – serine  
SI-1 – Src Inhibitor 1  
siRNA – small interfering RNA  
Src/ c-Src – cellular Src kinase  
SRM – selected-ion reaction monitoring  
TBST – Tris-buffered saline with Tween  
Thr/T – threonine  
TOF – time of flight  
Tyr/Y – tyrosine  
UPLC – ultra-performance liquid chromatography  
VH1 – vaccinia homolog 1  
VHR – vaccinia homolog-related  
WT – wild type  
YVH1 – yeast vaccinia homolog 1  
ZBD – zinc-binding domain

# CHAPTER 1: INTRODUCTION

## *1.1 Mass Spectrometry in Proteomics*

In the landscape of 21<sup>st</sup>-century molecular biology, the disciplines of biological mass spectrometry and proteomics have served as a necessary complement to genomic and transcriptomic knowledge bases and expanded our understanding of the human genome on a functional level. Biological mass spectrometry involves the identification, quantification, and characterization of proteins from a variety of biological contexts.<sup>2,3</sup> Since protein expression and modification processes are dynamically regulated to adapt to the homeostatic needs of the cell, the proteome is subject to constant change in response to various factors (growth, stress, etc.).<sup>3</sup> While this variability poses challenges, it is somewhat mitigated by modern developments in high-throughput methods such as mass spectrometry – allowing for increased sensitivity to identify protein-associated trends in response to experimental conditions.<sup>4</sup>

Mass spectrometry involves using instrumentation to deliver molecules into the gas phase, where they are ionized, separated, and detected on the basis of their mass-to-charge ratios ( $m/z$ ).<sup>5</sup> When analyzing proteins by mass spectrometry, the most common approach is through *bottom-up proteomics* – a method that involves a predictable enzymatic or chemical digestion of proteins in solution before their exposure to the mass spectrometer.<sup>6</sup> This process produces smaller molecules (peptides) that are better separated by chromatography and subsequently ionized more easily.<sup>6</sup> Fragments associated with these peptides are therefore representative of the native protein's

presence in a solution. Some proteomic applications of mass spectrometry include protein quantitation,<sup>7</sup> interactome analyses,<sup>8</sup> structural dynamics,<sup>9,10</sup> and elucidation of post-translational modifications.<sup>11,12</sup>

Mass spectrometers are composed of three primary components: an ionization source, a mass analyzer, and a detector.<sup>5</sup> The ionization source is the component required to convert analyte molecules into the gas phase and simultaneously ionize them, allowing them to travel through the instrumentation along an electrical field. The two most common types of soft ionization sources for the analysis of peptides are electrospray ionization (ESI) and matrix-assisted laser desorption/ionization (MALDI).<sup>5</sup> While MALDI uses a laser to vaporize and ionize solid, matrix-bound peptides,<sup>13</sup> ESI involves dispensing peptide solution from an electrically charged capillary where it is rapidly nebulized into the gas phase. This capillary carries a high voltage and temperature, which contributes to both the charge repulsion of peptides in solvent droplets, and a gradual decrease in droplet size. Eventually the repulsive forces between analyte molecules exceed the surface tension of the solvent (The Rayleigh limit) and eject the peptides, with any associated protons from the acidic solvent, into the gas phase in a “Coulombic explosion” (**Figure 1.1A**).<sup>5,14</sup> Since ESI uses aqueous samples, ESI mass spectrometers can be coupled to a liquid chromatography system (such as RPLC) to allow the researcher to gradually introduce analyte peptides in the order of their molecular properties (eg. decreasing hydrophobicity). This extra level of control provides better data resolution, as analyte peptides can now also be identified as a function of their chromatographic retention times.<sup>5,15</sup>

After peptides are ionized, they are subjected to mass analyzers that are responsible for separating the ions by their  $m/z$  ratios.<sup>5</sup> Although various technologies exist, two of the more relevant mass analyzers to this study are *quadrupole* and *time-of-flight* (TOF) mass analyzers. Quadrupoles operate as mass filters by creating an oscillating electrical field across two pairs of opposing electrodes. This field can be modulated by changing the radio frequency (RF) and direct current (DC) voltages of the poles to establish upper and lower  $m/z$  limits for ion transmission. Any “non-resonant” ions that possess a  $m/z$  ratio outside of this selected range are diverted away from the ion path and excluded from detection (**Figure 1.1B**).<sup>5,16</sup> On the other hand, TOF mass analyzers operate by rapidly accelerating ions into a “field-free” vacuum region, where all ions are granted equal kinetic energy.<sup>5</sup> As a result, ions of larger mass and lesser charge will travel slower through the TOF analyzer than smaller, highly charged ions. The detector then calculates the drift time of each ion as a function of its  $m/z$  ratio as they strike it (**Figure 1.1D**). Fundamentally, MS detectors serve to amplify these signals, and report each  $m/z$  ratio detected against its relative abundance in the sample (**Figure 1.1E**).<sup>5</sup>

### 1.1.1 Tandem Mass Spectrometry (MS/MS)

The detected  $m/z$  value of a *precursor ion* on a MS spectrum is insufficient information to conclude the identity of a peptide, and a more rigorous approach must be taken to sequence them. The solution to this problem lies in *tandem mass spectrometry*, or MS/MS. In MS/MS the instrument alternates between two modes during the continuous elution of a chromatographic peak to obtain  $m/z$  data of the intact peptide in one mode, and  $m/z$  values of its fragments (referred to as *fragment ions*) in the next.<sup>5</sup> The first mode, referred to as MS1, involves setting the first mass analyzer (usually a

quadrupole) to act as an ion guide. This delivers all precursor ions in a sample to the second mass analyzer (**Figure 1.1D**) to be detected whole, producing a spectrum that is referred to as an “MS fingerprint”. In the second mode, referred to as MS2, the first mass analyzer is now activated to select for ions within a defined m/z range (**Figure 1.1B**).<sup>5</sup> The m/z range selected is informed by the m/z values obtained in MS1, that correspond to peptides of interest. These ions are then transported from the mass analyzer to another compartment to undergo *collision-induced dissociation* (CID) – collisions with an inert gas to produce *fragment ions* of the selected precursor ion (**Figure 1.1C**).<sup>16</sup> The second mass analyzer is now utilized to resolve the fragment ions and produce a product ion spectrum. These experimentally obtained m/z values can be passed through a database search of predicted fragment ion m/z to verify peptide identity or any retained interactions or post-translational modifications.<sup>5,11</sup>

There are 2 different approaches to obtaining MS/MS data: *data-independent acquisition* (DIA) and *data-dependent acquisition* (DDA) modes. Data-independent acquisition involves the simultaneous MS/MS fragmentation and analysis of all peptides in a specified retention time or m/z range.<sup>17</sup> This method is optimal for proteome analysis studies, as it analyzes an entire data set free from instrumental bias. However, this comes at the cost of needing to use sophisticated data analysis software to deconvolute the resulting spectra.<sup>5,17</sup> Alternatively, data-dependent acquisition involves selecting precursor ions based on MS1-derived intensity data, followed by isolating and performing MS/MS analysis on the most abundant precursor ions detected in the sample. This allows for characterization of relatively abundant peptides in a sample and is

particularly useful when searching for post-translational modifications in proteins that have been previously analyzed via MS.<sup>5</sup>

When applied to biological systems, the high-throughput nature of mass spectrometry can be wielded to process large amounts of proteomic data on dynamic, cellular environments.<sup>4</sup> The advent of label-free quantitation and targeted MS techniques have paved the way to accurately assess the minute detail in which proteins associate with each other, regulate each other, and therefore sustain life.

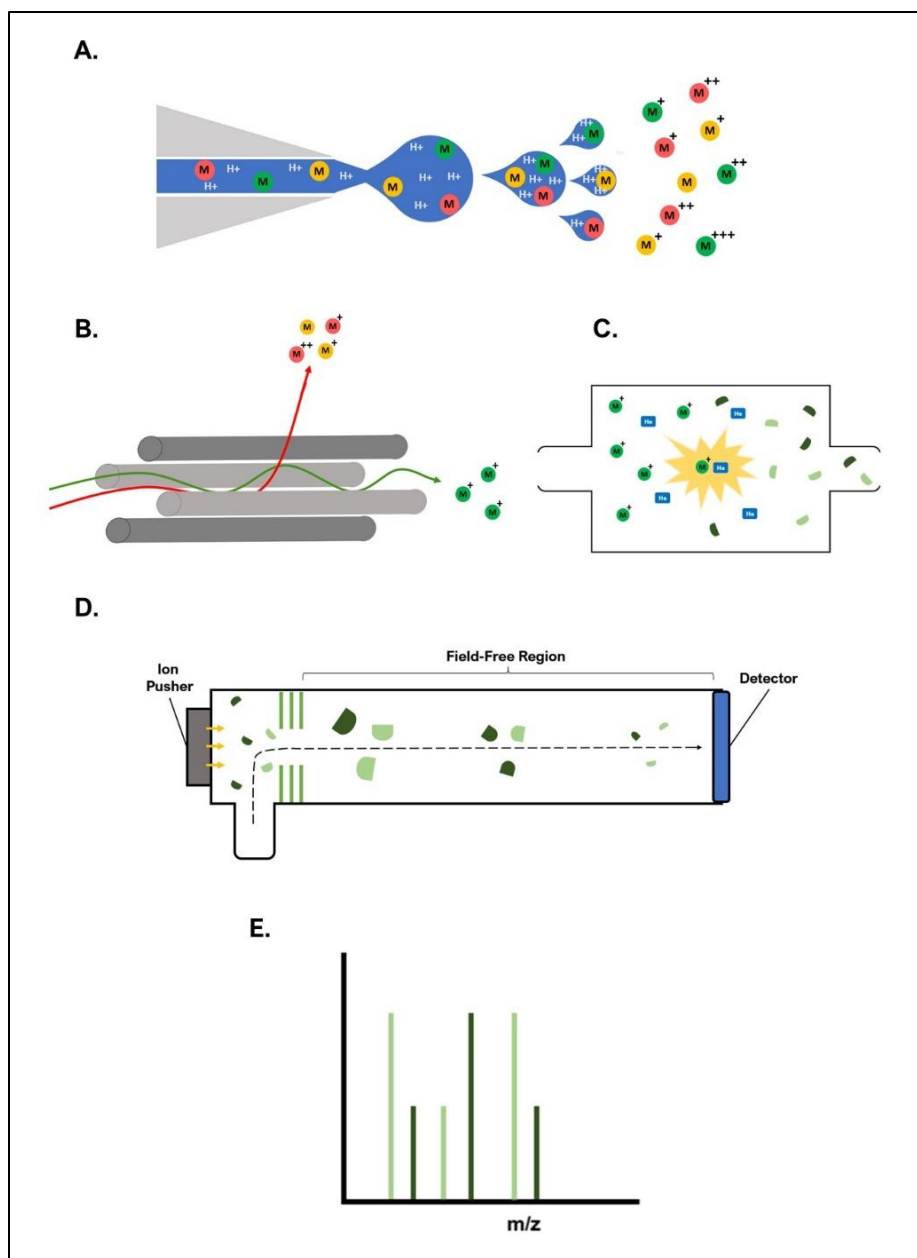


**Figure 1.1 Schematic of vital components in a mass spectrometer.** **A)** A demonstration of electro spray ionization (ESI), outlining the droplet shrinking, and Coulombic explosion that results in analyte molecules abstracting protons from the acidic solvent. **B)** A quadrupole acting as a mass filter, only allowing molecules of a specific  $m/z$  to pass through and diverting non-resonant molecules away from detection. **C)** A collision cell, outlining the fragmentation of precursor analyte molecules by collision with helium. **D)** A time-of-flight tube (TOF), demonstrating the acceleration of fragment ions by the ion pusher, into a field-free region that is under vacuum. All fragments are given the same kinetic energy, but the smallest molecules with the highest charge will move fastest. The ion path is outlined by the dotted line. **E)** A sample MS/MS spectrum, with ion  $m/z$  plotted on the x-axis and ion abundance plotted on the y-axis.

## ***1.2 Reversible Protein Phosphorylation Dynamics***

Many proteins within cellular systems are structurally and functionally regulated by the covalent addition of chemical functional groups, in a process known as post-translational modification (PTM).<sup>18</sup> While products of ribosomal translation may receive a variety of modifications – such as methylation,<sup>19</sup> acetylation,<sup>20</sup> glycosylation,<sup>21</sup> and ubiquitination<sup>22</sup> – the most widespread PTM within the cell is thought to be phosphorylation.<sup>12,23</sup> It is estimated that thirty percent of all proteins are subjected to phospho-regulation at a given moment.<sup>24,25</sup>

Protein phosphorylation and dephosphorylation are best conceptualized by examining two types of enzymes: kinases and phosphatases. Phosphorylation is performed by kinase enzymes, which transfer the  $\gamma$ -phosphate of ATP to an available hydroxyl group on a protein.<sup>18</sup> These targeted hydroxyl groups are most often located on the side chains of Ser, Thr, and Tyr amino acid residues.<sup>24</sup> In the opposing process of dephosphorylation, phosphatase enzymes abstract the phosphate group from a previously phosphorylated site and subsequently regenerate the hydroxyl group of the target. **(Figure 1.2).**<sup>18</sup>

The joint processes of phosphorylation and dephosphorylation are leveraged to control a variety of intracellular phenomena – such as signal propagation,<sup>26</sup> subcellular localization,<sup>27</sup> molecular degradation,<sup>28</sup> and enzyme activation and deactivation<sup>18</sup> – to name a few. The regulation of enzyme activity is one particularly noteworthy application of phosphorylation. On a structural level, there are electrostatic and steric implications of inserting a negatively charged tetrahedral ion on a protein surface that is laden with other charged groups. This then leads to conformational change within the protein, as the

structure is altered to accommodate the attractive and repulsive interactions between the newly introduced phosphate group and the surrounding structural elements of the target protein.<sup>29</sup> The result is a reconfigured enzyme that may have gained or lost access to a substrate or key regulatory factor that is required for catalysis.<sup>18,29</sup>

Despite the harmonious relationship between these two types of enzymes to maintain homeostasis at the molecular level, states of regulatory dysfunction may occur, and consequently lead to biological disease. Kinase and phosphatase dysregulation have been implicated in a wide variety of human illnesses, including neurological diseases, metabolic disorders, cardiovascular diseases, and numerous forms of cancer.<sup>25,30,31</sup> It is for this reason that researchers continue to study phosphorylation patterns in association with a disease phenotype of interest.

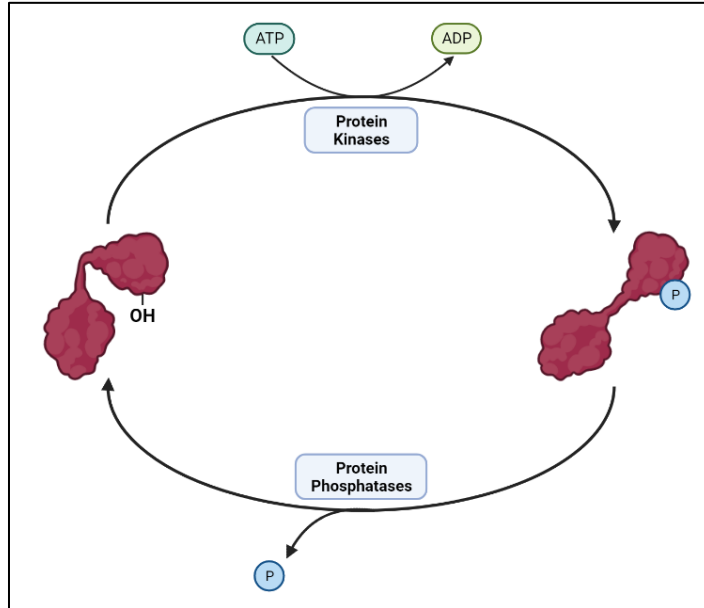


**Figure 1.2 Protein Phosphorylation and Dephosphorylation.** The synergistic relationship of kinases and phosphatases. Kinases catalyze the transfer of a phosphate group from ATP to a free -OH group on an enzyme, producing ADP in the process. Phosphatases may then hydrolyze the phosphate to remove it from the enzyme, producing inorganic phosphate.

### ***1.3 Tyrosine Phosphatases and the PTP Superfamily***

The characterization of kinase and phosphatase enzymes began in 1955 with the discovery of the first kinase, “phosphorylase kinase” and phosphatase, “phosphate-releasing enzyme” (now known as PP1).<sup>32</sup> In the following decades, kinase research became the focus of phosphorylation studies – while phosphatases were largely regarded as indiscriminate “housekeeping” enzymes. This research trend continued until 1992, when Fisher and Krebs received the Nobel prize for their discovery of reversible protein phosphorylation, which underscored the regulatory importance of phosphatases.<sup>33</sup> Since then, studies examining numerous phosphatase families have taught scientists that the dephosphorylation component of reversible protein phosphorylation required analogous specificity and regulatory control, requiring comprehensive characterization of the enzyme families that mediate dephosphorylation of biomolecules.

Interestingly, approximately ninety-eight percent of all protein phosphorylation events in the cell take place on Ser and Thr residues, and only about two percent occur on Tyr residues.<sup>25,34</sup> Despite such a low fraction of endogenously phosphorylated Tyr residues, the Protein Tyrosine Phosphatase (PTP) superfamily is disproportionately larger than the Protein Serine/Threonine Phosphatase superfamily (PSP) – with more than threefold the number of enzymes.<sup>35,36</sup> A closer look at the PTP superfamily reveals that the PTPs consist of a greater diversity of phosphatase enzymes all sharing a common structure and catalytic mechanism.<sup>25,34</sup>

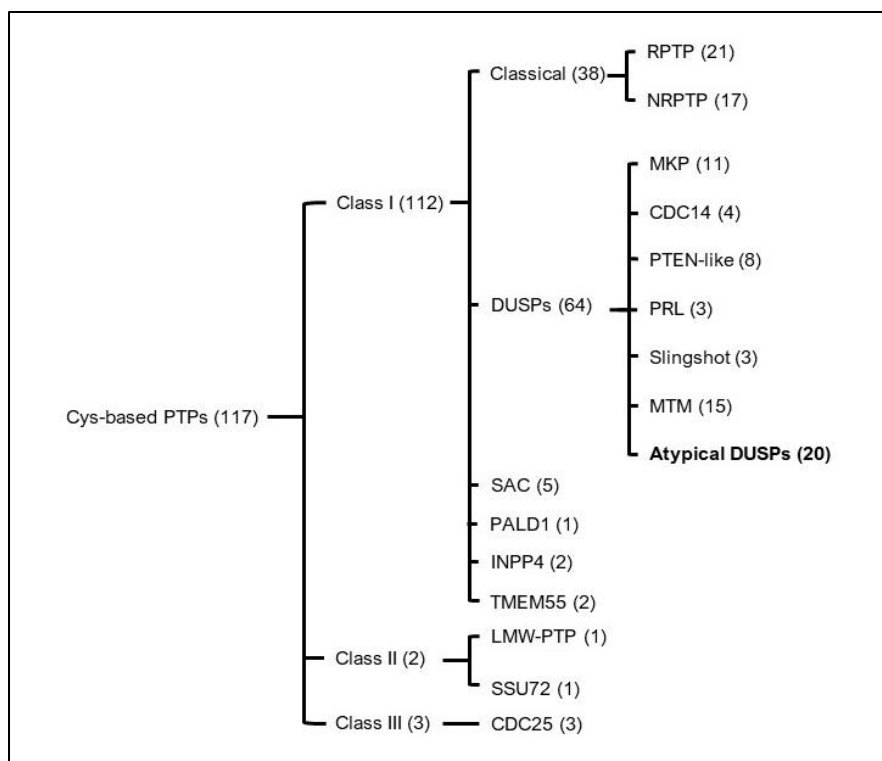


**Figure 1.3. The Cys-based PTP superfamily.** A phylogenetic tree displaying the relationship of Cys-based PTPs. Class II and III PTPs constitute 3 families, with a collective 5 enzymes between them. Class I PTPs possess several subclassifications, the largest of which are the classical “Receptor-like” and “Non-receptor-like” PTP subfamilies and the VH1-like or “DUSP” subfamily. The DUSPs are further subdivided into the MAP kinase phosphatases, Slingshots, Phosphatases of the regenerating liver, Cell Division Cycle 14, PTEN-like, myotubularin, and atypical DUSP subfamilies. Adapted from Tautz et al.<sup>25</sup>

PTPs are characteristically defined by a consensus HCX<sub>5</sub>R(S/T) sequence located in a region in the active site known as the phosphate-binding loop, or “P-loop”.<sup>34</sup> As the name suggests, this motif is responsible for binding phosphate moieties – and it does so through formation of a thiophosphate intermediate by an invariant, catalytic Cys residue.<sup>34</sup> This Cys residue notably can act as a nucleophile, as its pKa is decreased by its proximity to the imidazole group of the P-loop His and the inwardly-projecting amino groups of the polypeptide backbone.<sup>25,34</sup> The PTP mechanism proceeds through 2 steps (see Figure 2); in the first step, the Cys residue performs a nucleophilic attack on the

phosphorus atom, creating a transition state that is stabilized by the aforementioned Arg. An Asp residue in proximity then performs the hydrolysis of the phosphate group from the substrate to form the thiophosphate intermediate, and subsequent release of the substrate. The second step of the mechanism involves the use of an ordered water molecule, coordinated by a nearby residue (usually Gln). The Asp residue, now deprotonated, abstracts a proton from the ordered water molecule and allows the hydrolysis of the phosphoester bond and rapid ensuing regeneration of the enzyme.<sup>25,34</sup>

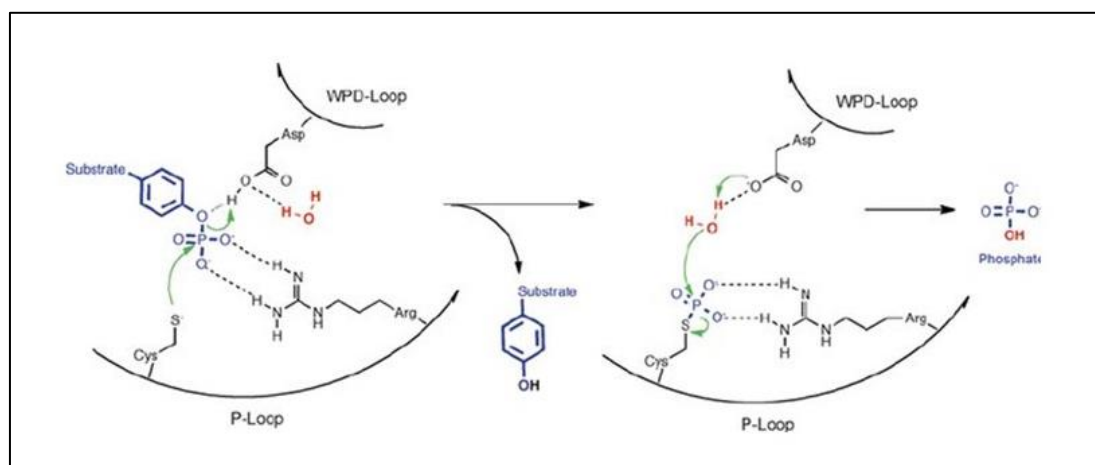


**Figure 1.4. The PTP catalytic mechanism.** The 2-step mechanism by which all Cys-based PTPs operate. The first step (pictured left) involves the nucleophilic attack of the P atom by the catalytic Cys, followed by hydrolysis of the phosphodiester bond by an Asp to release the substrate. The second step (pictured right) shows the regeneration of the enzyme via abstraction of a proton from the ordered water molecule by the Asp, and subsequent hydrolysis of the thiophosphate intermediate. Figure obtained from Tautz et al.<sup>25</sup>

There are 117 Cys-based members of the PTP superfamily, divided into 3 subclasses numbered I-III.<sup>25,34</sup> The majority of PTPs can be found in Class I, which is further subdivided into classical PTPs and the “VH1-like” or “Dual Specificity Phosphatases” (DSPs or DUSPs). The DUSP subfamily is intriguing as they possess characteristically shallower binding pockets, allowing them to also dephosphorylate Ser

and Thr residues, in addition to Tyr. There are many different enzyme subclassifications within the DUSP family, such as the MKPs, the PRLs, the slingshots, the CDC14s, the PTENs, and the myotubularins.<sup>25</sup> There is also one other recognized category of DUSP, the atypical DUSPs, which lack easily recognizable structural motifs that would indicate specific, well-characterized molecular interactions (such as the N-terminal CH2 domain present in MKPs).<sup>25</sup> The first identified DUSP, a viral phosphatase called VH1, belongs to this category of poorer-characterized and less functionally related enzymes.<sup>37</sup>

#### ***1.4 The Yeast Phosphatase: YVH1***

One of the earliest identified atypical DUSPs, the yeast YVH1's discovery predated the now-conventional DUSP family nomenclature. In 1992, Guan and Dixon discovered a novel PTP in *S. cerevisiae* that shared sequence homology with the viral VH1 phosphatase. As a nod to its evolutionary lineage, it was designated YVH1.<sup>38</sup> However, YVH1 has several prominent structural and functional differences from VH1. This is first evident in its size; YVH1 is a 364 amino acid protein, while VH1 is only 171 amino acids long.<sup>37,38</sup> The approximate doubling of its length is attributed to a novel C-terminal, Zn-binding domain (ZBD) present in YVH1. For this reason, sequence homology between VH1, YVH1, and other early-identified DUSPs (such as the murine MKP-1, "3CH134") is restricted to the phosphatase domain.<sup>37-39</sup>

The phosphatase activity of YVH1 also differs greatly from VH1. In phosphatase assays, YVH1 demonstrated some rudimentary phosphatase activity against artificial substrates. This contrasts with VH1, which possesses ~200x more catalytic activity than

YVH1.<sup>38</sup> Despite the catalytic inefficiency of YVH1, it is remarkable that most of the residues required for catalysis are invariant to VH1 – with the active site showing the most conservation.<sup>38</sup>

YVH1 also has many phenotypic implications on yeast biology. Upon inactivation of the YVH1 gene, yeast spores still showed vegetative growth, but these mutant colonies displayed 3x longer doubling times. This phenotype (referred to as *slow growth* in literature) was not linked to arrest at a stage of the cell cycle though, as would be expected in CDC protein mutants.<sup>38</sup> Alternatively, steady-state YVH1 gene expression was induced by nitrogen starvation, pointing to a role in nitrogen metabolism in yeasts.<sup>38</sup>

### ***1.5 The Human Phosphatase: hYVH1***

A human orthologue of YVH1 was discovered in 1999 with 31% sequence identity to its yeast counterpart and was dubbed hYVH1 (later designated as DUSP12).<sup>1</sup> Consistent with the trend initially observed in the yeast model – there are no known hYVH1 paralogs in the human genome, with the only gene copy mapped to chromosome 1q21-q22. Curiously, this region of the genome is highly expressed in various human cancers,<sup>40-42</sup> which may suggest a selective pressure to restrict gene duplication. However, this singular gene copy has been conserved throughout eukaryotic evolution (**Figure 1.5**), which may be suggestive of an indispensable cellular function.<sup>1</sup>

The *hyvh1* gene codes for a protein 340 amino acids long that is composed of two distinct domains: an N-terminal phosphatase domain, and a cysteine-rich, C-terminal, Zn-binding domain (ZBD; **Figure 1.6**). These domains are approximately equal in size and

are separated by a short, intrinsically disordered “linker” region.<sup>1</sup> The phosphatase domain’s active site possesses the HCX<sub>5</sub>R(S/T) motif that is characteristic of all PTPs, as well as differences that are consistent with a DUSP catalytic domain – such as the shallower GX<sub>5</sub>S binding pocket motif to accommodate Ser/Thr association, and lack of the hinged WPD-loop that swings the catalytic acid into position.<sup>1,34</sup> Despite these accommodations for dual specificity, hYVH1 still displays an extreme preference for pTyr.<sup>1</sup> Being an atypical DUSP, the catalytic domain lacks easily recognizable motifs that would implicate it in well-defined functional interactions, like the aforementioned CH2 domain.<sup>1,34</sup> Furthermore, there has been no identified biological substrate that directly associates with – and is dephosphorylated by – the catalytic domain of hYVH1.



**Figure 1.5. Sequence alignment of hYVH1 and YVH1 orthologues.** A sequence alignment of hYVH1 and orthologues, adapted from Muda et al.<sup>1</sup> N-terminal catalytic domain is outlined in red, C-terminal ZBD is outlined in green. Conserved Cys and His residues are highlighted in yellow. The active site Cys is highlighted in red. General amino acid conservation and functional conservation are outlined in respective colours.

Like its yeast ancestor, the phosphatase domain displays significantly less catalytic efficiency than the prototypical human VHR (DUSP3) model when presented with a generalized phospho-substrate.<sup>43,44</sup> Unlike VHR and most traditional DUSPs, hYVH1 is far more resilient to mounting oxidative stress, and resultant oxidative inactivation of its catalytic Cys.<sup>43</sup> This is due to the ability of the Cys-rich, Zn-binding domain to function as a redox sensor by having its cysteines favourably oxidized in place of the catalytic Cys (C115), and by also forming protective, intramolecular disulfide bonds with the catalytic Cys – thus shielding it from oxidative inactivation.<sup>45</sup>

Findings such as this have made the Zn-binding domain a fascinating element of hYVH1's biochemistry. The ZBD is structurally defined by its ability to coordinate 2 moles of Zn per mole of protein through 7 evolutionarily invariant Cys residues, collectively forming two Zn-finger motifs.<sup>45</sup> Within the PTPs, this domain remains exclusive to hYVH1,<sup>34</sup> and the majority of the observed functions of hYVH1 are contingent on the presence of the ZBD.<sup>43,45-47</sup> This observation persists in the yeast model as well, as the slow growth phenotype initially observed in YVH1-silenced yeast was reverted by insertion of an hYVH1 expression vector – but only if the ZBD had not been removed via mutation.<sup>1</sup> This underscores both the importance of the ZBD, as well as its functional conservation.

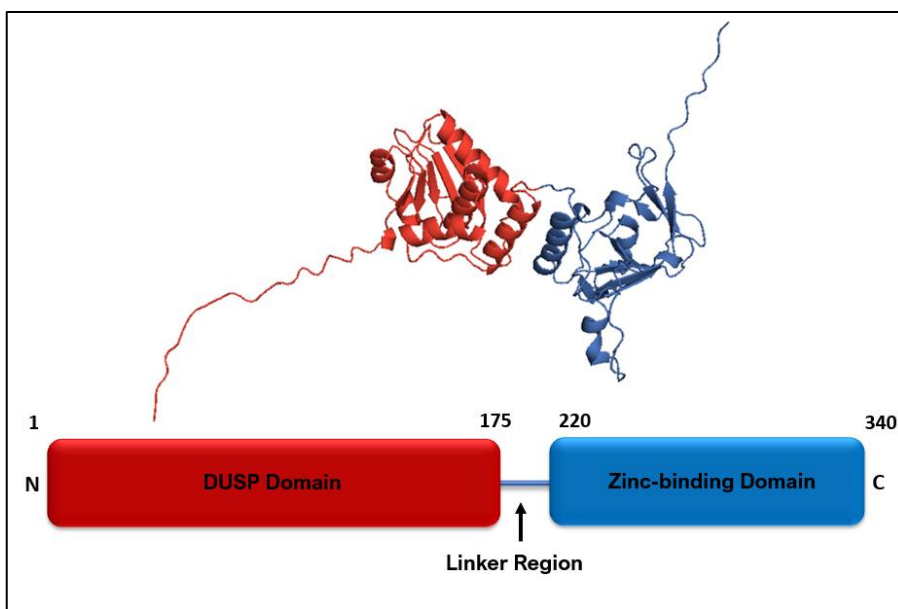


**Figure 1.6. The domain structure of hYVH1.** A predictive model of hYVH1 assembled through SwissMODEL by integrating X-ray crystallography data for the N-terminal DUSP domain (red), with a CryoEM structure for the ZBD (blue).<sup>48</sup> The structure was formatted in PyMOL.<sup>49</sup>

Pertaining to human models, hYVH1 has been demonstrated to play a role in a variety of cellular functions. With regards to the cell cycle, overexpression of hYVH1 has been linked to increased progression from the G0/G1 to the G2/M stage of cell division, as well as an increase in multinucleated, polyploid cells.<sup>46</sup> Conversely, siRNA silencing of hYVH1 expression leads to cell cycle arrest at the G0/G1 stage, and eventual senescence. This was also an observation attributed to the ZBD, and it was deemed “necessary and sufficient” for cell cycle progression.<sup>46</sup> Despite these findings, hYVH1 has been more extensively studied in its roles in cell survival,<sup>43,50</sup> stress granule disassembly,<sup>47</sup> and ribosome biogenesis.<sup>51</sup>

## ***1.6 hYVH1 in Cell Survival***

One of the most intriguing roles attributed to hYVH1 to date is its function as a cell survival factor. Complementary to its observed catalytic resilience to oxidative stress, our lab demonstrated that overexpression of hYVH1 increases cell survival when compared to WT cells under oxidative and heat-shock stress conditions.<sup>43</sup> Neither catalytically dead hYVH1 (C115S mutant) or ZBD-deleted hYVH1 can exert the same cytoprotective effects, suggesting that both are required for this function.<sup>43</sup>

Our lab has also recently shown that hYVH1 has a functional role in stress recovery by contributing to stress granule disassembly in response to arsenic-induced oxidative stress.<sup>47</sup> Stress granules are ribonucleoprotein (RNP) structures consisting of mRNA and proteins that form under cellular stress to preserve their constituent materials for later translation.<sup>52</sup> During recovery from arsenic-induced stress, hYVH1 overexpression resulted in a decrease in stress granule size, whereas silencing of the *hyvh1* gene impaired stress granule dissociation. This stress granule connection was originally observed through colocalization with several RNPs during arsenic stress recovery, including Y box-binding protein 1 (YB-1) and fragile X mental retardation protein (FMRP).<sup>47</sup> Both have been previously characterized as translational repressors, and stress granule markers.<sup>53</sup> Another protein that plays a role in stress granule disassembly and has separately demonstrated binding interactions with hYVH1 is the molecular chaperone, Hsp70.

### 1.7 Hsp70 and the association to hYVH1

The 70kDa Heat Shock Protein (Hsp70) is a molecular chaperone that is a vital housekeeping enzyme. Its primary functions include assisting in *de novo* folding of nascent polypeptide chains into functional proteins, solubilizing and refolding aggregated and denatured proteins back to their native state, membrane translocation, and control of regulatory elements responsible for processes such as protein degradation and apoptosis.<sup>54,55</sup> Hsp70 is upregulated under general stress conditions, as cells display increasing reliance on it to exert its anti-apoptotic and cytoprotective effects.<sup>54</sup> This demonstrates the pathological relevancy of Hsp70, which shows high abundance in various cancers and is correlated to chemotherapy resistance.<sup>56</sup> On the other hand, Hsp70 is shown to be under-expressed in neurodegenerative disorders, contributing to low cell survivability and characteristic disease phenotypes.<sup>54</sup>

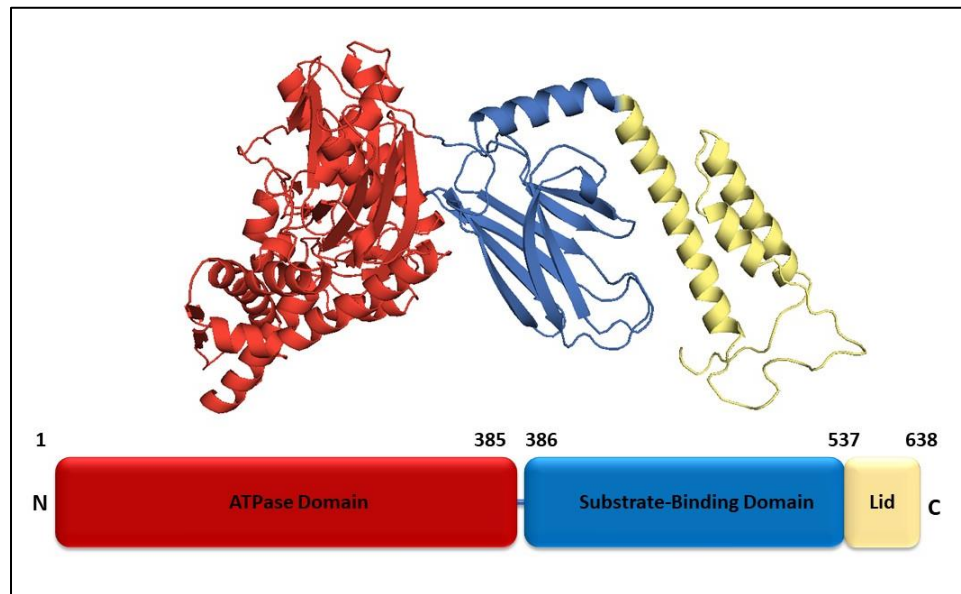


**Figure 1.7. Domain Structure of Hsp70.** X-ray crystallography structure of Hsp70, displaying N-terminal ATPase domain (red) and C-terminal Substrate-binding domain (blue), separated by a short linker region. The C-terminal domain is further subdivided, highlighting the helical lid subdomain (yellow) that folds over a substrate binding pocket. The structure was formatted in PyMOL.<sup>49</sup>

On a structural level, Hsp70 consists of 2 domains: a 45kDa N-terminal ATPase domain, and a 25kDa substrate binding domain that also features an indispensable “Lid” subdomain (**Figure 1.7**).<sup>54</sup> Due to its role as a molecular chaperone, Hsp70 accordingly has myriad binding partners, most of which interact with its substrate-binding domain to engage with it for structural recovery. Hsp70 binds substrates to its substrate-binding domain in accordance with its ATPase domain cycle. When the ATPase domain of Hsp70 is bound to ATP, the protein displays a low affinity for substrates and fast substrate exchange rates; at this point a substrate will bind, ATP is hydrolyzed to ADP, and the substrate-binding domain changes to a higher-affinity state to perform its chaperone functions.<sup>54</sup> Most proteins that interact with the ATPase domain of Hsp70 perform a regulatory function related to its chaperone activity, and are often referred to as co-chaperones.<sup>57</sup> This creates a distinction between unfolded proteins that are bound by Hsp70 for a chaperone function, and proteins that interact with it in a regulatory fashion to control Hsp70’s activity or localization.

It is with this understanding of Hsp70, that the association between hYVH1 and Hsp70 is significant. It was observed through reciprocal pulldown experiments involving endogenous protein or overexpressed variants, that hYVH1 can co-precipitate Hsp70, as well as a mutant of Hsp70 consisting of only the N-terminal ATPase domain. This association is contingent on the entire hYVH1 protein being intact, as removal of either domain abrogates the interaction.<sup>43</sup> Within a cellular context, co-immunofluorescent microscopy experiments determined that the endogenous proteins co-localize to the perinuclear region in response to heat shock stimulation. Overexpression of each protein independently increases the overall survivability of cells under peroxide and heat-shock

induced stress.<sup>43</sup> However, co-expression of hYVH1 and Hsp70 has been shown to further increase cell survivability, suggesting the hYVH1-Hsp70 complex represents a potent cytoprotective factor during response to these cellular insults.<sup>43</sup>

### ***1.8 Src Kinase and hYVH1***

c-Src (referred to here as simply Src) was one of the first identified proto-oncogene in humans, and codes for a protein 536 amino acids in length (~60 kDa in mass). It is a non-receptor tyrosine kinase that serves roles in cell cycle regulation, cell proliferation, differentiation, and apoptosis among other functions.<sup>58</sup> Based on this information, it is unsurprising that dysregulation of Src leads to anchorage-independent cell growth *in vitro* and tumor development *in vivo*.<sup>59</sup>

Structurally, Src is composed of 5 notable regions: an N-terminal “unique” domain (showing poor conservation), an SH3 domain that lends itself to aromatic stacking interactions, a phosphotyrosine binding SH2 domain, a tyrosine kinase catalytic domain, and a short C-terminal region that possesses a highly conserved Tyr residue.<sup>59</sup> When this tyrosine (Tyr 530) is phosphorylated, the catalytic domain of Src is functionally inactive due to an intramolecular conformational change that is mediated by the SH2 domain of Src associating with the phosphorylated Tyr530. The most prevalent oncogenic mutations in Src kinase are mutations that disrupt this autoinhibitory interaction, resulting in a constitutively active kinase that possesses oncogenic potential.

58,59

Previous hYVH1 interactome analyses by our lab had identified an association with Src in a subset of biological replicates. It was later determined that hYVH1 was a target for direct Src phosphorylation, with a phospho-site on hYVH1 mapped to Tyr179 in the linker region between the DUSP domain and ZBD.<sup>51</sup> With the observed formation of the hYVH1-Hsp70 complex, a following study by our lab had determined that co-expression of Src alongside hYVH1 and Hsp70 resulted in abrogation of the hYVH1-Hsp70 interaction.<sup>60</sup> Src has also been shown to alter the 80S proteome when co-expressed alongside hYVH1, demonstrating the potential relevance of this interaction in ribosome biogenesis.<sup>51</sup>

### ***1.9 Ribosome Biogenesis and hYVH1***

One of the most vital pieces of intracellular machinery is the ribosome – a ribonucleoprotein complex composed of rRNA and protein that is responsible for translation of mRNA into polypeptides. Eukaryotic ribosomes are composed of a smaller 40S subunit that interacts with mRNA for translation initiation and codon alignment, and a larger 60S subunit that catalyzes peptide bond formation in nascent polypeptide chains.<sup>18</sup> Both subunits are manufactured independently in the nucleus and associate together after independent shuttling to the cytoplasm. However, the nuclear export and association of the two ribosomal subunits is a sophisticated and tightly coordinated process that involves the association and dissociation of over 150 transacting factors to produce a translationally fit ribosome.<sup>61</sup> These shuttling proteins are often recycled back into the nucleus after dissociation to perform another cycle of ribosome biogenesis. If these transacting factors are impaired in their ability to re-localize to the nucleus, the

ensuing decline in their nuclear availability may result in nuclear export failure and a deficit of translationally competent ribosomes.<sup>61</sup>

Implication of YVH1 orthologs participating in ribosome biogenesis was first observed in yeast. Yeast strains lacking the *yvh1* gene display a decrease in translationally competent 80S ribosomal species, and increased sequestering of pre-60S subunits in the nucleus.<sup>61</sup> The consequence of this was the development of 43S ribosomal “halfmers” – 40S subunits with necessary initiation factors and an mRNA positioned at the start codon, awaiting 60S association to begin translation. Follow-up experiments to determine where YVH1 acts in the ribosome biogenesis cascade demonstrated that YVH1 is required to bind to the pre-60S subunit in the nucleus, to release the placeholder protein Mrt4 from the subunit and allow for the binding of the P<sub>0</sub> stalk protein (also known as uL10) in its place.<sup>61,62</sup> This is one of the final steps in 60S ribosome biogenesis, as P<sub>0</sub> allows for the formation of the ribosomal stalk complex and the ensuing association of the 60S subunit to the 40S subunit to form a mature 80S complex.<sup>62</sup>

### *1.9.1 hYVH1 and Src at the 80S ribosome*

One of the observed effects of Src phosphorylation of hYVH1 at Tyr179 was the increase in nuclear localization of hYVH1.<sup>51</sup> Within the context of ribosome biogenesis, this observation suggested that Src may be responsible for recycling hYVH1 back to the nucleus after hYVH1 is displaced from the 60S subunit.<sup>51</sup> Phosphorylation at Tyr179 also led to a decrease in hYVH1 localization to stress granules.<sup>60</sup> Ribosomal profiling experiments determined that Src co-expression with hYVH1 resulted in an increase in

polysomes (multiple ribosomes that are bound to and actively translating a single mRNA) and translationally available monosomes.<sup>51</sup> It also caused a decrease in translationally stalled intermediates known as *disomes*, hypothesized to be a consequence of ribosomal hibernation (particularly in conditions of stress)<sup>63</sup> or a collision of two ribosomes translating the same mRNA.<sup>64</sup> A following quantitative proteomic analysis discovered hYVH1-Src co-expression significantly decreased the levels of several translational repressors at the monosome/disome. In contrast, co-expression of hYVH1-Src increased the levels of proteins at the monosome/disome that are involved in translational efficiency, such as eukaryotic initiation factor 6 (EIF6), elongation factor 2 (EF2), and receptor for activated C kinase (RACK1).<sup>51</sup> The increase in EIF6 is particularly intriguing as this molecule has been characterized as an anti-association factor for subunit joining. EIF6 is thought to serve as a critical checkpoint function for increasing translational efficiency and reducing dysfunctional ribosome formation.<sup>65</sup>

### ***1.10 Objectives***

With demonstrated functions in ribosome biogenesis,<sup>51</sup> stress resistance,<sup>43,45</sup> and cell cycle regulation,<sup>46</sup> there is merit in investigating the mechanistic details of hYVH1's protein-protein interactions. While there is evidence that shows phosphorylation of Tyr179 as a regulator of hYVH1's localization,<sup>51</sup> preliminary data shows that Tyr179 phosphorylation is not responsible for mediating the association to Hsp70, suggesting additional Src-mediated phosphorylation sites are present on hYVH1. Furthermore, the binding interface between Hsp70 and hYVH1 is still poorly understood. Advance knowledge of how hYVH1 associates with Hsp70 may deepen our understanding of the structural mechanism of Src-mediated attenuation of the hYVH1-Hsp70 complex during basal conditions and in response to cell stress.

**The objectives are as follows:**

- 1) Examine the Src-hYVH1 phosphorylation event at the endogenous level.**
- 2) Identify the molecular determinants of hYVH1 association with Hsp70 using structural mass spectrometry.**
- 3) Map additional Src-mediated phosphotyrosine sites on hYVH1 using high resolution targeted mass spectrometry.**

## CHAPTER 2: MATERIALS AND METHODS

### 2.1 Plasmids

A wild-type (WT) FLAG-hYVH1 cDNA plasmid construct described by Muda et al.<sup>1</sup> was used for several experiments in this study, along with several cDNA mutant derivatives of this plasmid. These are: FLAG-hYVH1 Y179F, produced by Dr. Christopher Bonham; FLAG-hYVH1  $\Delta$ ZBD, produced by Dr. Qiudi Geng; and a novel FLAG-hYVH1 Y35E mutant generated through PCR-facilitated, site-directed mutagenesis with the Q5 site-directed mutagenesis kit (New England Biolabs). For this mutant, the generated forward primer was: 5'-TGCAGCCAGGATTGGAGTTCGGTGGGGCCGC-3', and the reverse primer was: 5'-GCGGCCCCACCGAACTCCAATCCTGGCTGCA-3' (BioBasic). The PCR product was sequenced by automated DNA sequencing, performed by GENEWIZ (Azenta). A human His<sub>6</sub>-Hsp70 plasmid was generously provided by Dr. Frank Sharp (UC Davis), and a human Myc-Src Y530F mutant plasmid was generously provided by Dr. Michel Tremblay (McGill University).

### 2.2 Cell Culture

HeLa cells (ATCC) were cultured in an adherent monolayer with 10mL of Dulbecco's Modified Eagle's Medium (DMEM) /Nutrient Mixture F12-Ham (Sigma), mixed with 10% fetal bovine serum (FBS; Gibco) and 1% penicillin-streptomycin antibiotic (Pen/Strep; Gibco). Passages were performed regularly to maintain ~70%

confluency by washing cells in PBS (Sigma) before lifting in 1mL of trypsin (SAFC), and resuspending in 9mL of DMEM. Cells were killed and re-plated from -80°C stocks after approximately 20-25 passages. Cells were counted and passaged 24 hours prior to transfection to obtain populations of ~1 million cells per plate.

Protein overexpression was performed via PEI-mediated transient transfection. Cell media was exchanged for antibiotic-free DMEM with 10% FBS. PEI and DNA plasmids were equilibrated in 150mM NaCl for 10 minutes. DNA and PEI solutions were then combined in a ratio of 1:3µg DNA:PEI and incubated for another 10 minutes before addition to plates. Plates were exchanged back into antibiotic-containing media after 6 hours. Cells were lysed 24 hours after transfection in a 50mM Tris-HCl lysis buffer (pH 7.4, 150mM NaCl, 1% Triton X-100 and 0.1% SDS) – supplemented with 10µg/mL Aprotinin (Sigma) and 0.5mM phenylmethylsulfonyl fluoride (PMSF; Sigma) as protease inhibitors. Cell plates were scraped and incubated on ice for 5 minutes, before centrifugation at 24,000 x G for 10 minutes. The supernatant was retained as soluble lysate, and the pellet was discarded.

For endogenous Src phosphorylation experiments, two 15cm plates of 2.5 million cells were grown for each sample. After 24 hours, the media was exchanged for serum-free media, and incubated for another 24 hours. Prior to lysis, all cells were stimulated with fresh DMEM containing 10% FBS, supplemented with 1mM pervanadate for 1 hour. During this hour, Src-inhibited samples received 20µM of Src Inhibitor 1 (SI-1; MedChemExpress) and uninhibited samples received an equivalent volume of DMSO. In the final 20 minutes of this incubation, each plate was administered 10ng/mL of

epidermal growth factor (EGF). During lysis, lysis buffer was supplemented with 1mM pervanadate and 1mM NaF.

### **2.3 Affinity Chromatography**

For pulldowns of FLAG-hYVH1, Anti-FLAG M2 Magnetic Beads (Sigma) were equilibrated by washing twice with the previously described lysis buffer. Cellular lysates were then added to the beads and incubated on a nutator for 3 hours to overnight at 4°C. After incubation, beads were washed three times with 50mM Tris-HCl wash buffer (pH 7.4), containing 150mM NaCl and 0.1% Triton X-100. This process was also used for pulldown of His<sub>6</sub>-Hsp70 with His-Mag Agarose Beads (Novagen), except a 1.5-hour incubation was performed in place of a 3-hour incubation. For the immunoprecipitation (IP) of endogenous hYVH1, a rabbit anti-hYVH1 antibody (provided by Dr. Jack Dixon) was prebound to Protein A Mag Sepharose beads (Cytiva) by incubating for 30 minutes on a nutator at room temperature, at a 1:10 antibody: bead ratio. This resin was then washed of unbound antibody with lysis buffer, and incubated overnight with cellular lysates on a nutator at 4°C.

For alkaline phosphatase treatments, Plates of 1 million cells were transfected with either 4μL hYVH1 + 1μL empty vector (EV), or 4μL hYVH1 + 1μL Src. Prior to lysis, cell media with 20mM of sodium orthovanadate was applied to cells for 90 minutes. Cells were lysed and IP was performed as described. After the third wash, the resin was equilibrated with two washes of a 50mM Tris-HCl buffer (pH 7.9) containing 100mM NaCl, 10mM MgCl and 1mM DTT. Beads were then resuspended in 500μL of

this buffer, supplemented with seven units each of calf intestinal phosphatase (CIP; Promega), and incubated overnight at 37°C. Resin was washed three times in this buffer, then administered SDS loading dye for western blots.

## **2.4 Mass Spectrometry Sample Preparation and Analysis**

Washed beads were transferred to siliconized microcentrifuge tubes (FisherScientific) then subjected to two more washes in PBS, followed by two washes in 50mM ammonium bicarbonate (AB). Beads were then resuspended in 50uL of 6.5ng/μL Sequencing Grade Modified Trypsin (Promega) in 50mM AB and digested overnight at 37°C in a shaking incubator. The digest was then quenched by addition of 100μL of Burdick and Jackson water (B&J; Honeywell), boiled at 95°C for 5 minutes, and then further diluted by the addition of another 100μL of B&J water. The beads were then magnetized as the solvent was transferred into a fresh siliconized tube and concentrated through a speed vacuum to a volume of ~25-50μL. Peptides were then reduced by the addition of 100μL of 10mM DTT (prepared fresh from a 50mM stock), and subsequent incubation on a microcentrifuge tube shaker for 45 minutes at room temperature. Alkylation was performed by adding 100μL of 20mM iodoacetamide (prepared from a fresh 50mM stock solution) and then incubation while shaking for 1 hour at room temperature, in the dark. Unreacted iodoacetamide was quenched by the addition of 20uL of 50mM DTT. The samples were then concentrated to ~50μL and resuspended in 100uL of 0.1% mass spectrometry-grade formic acid (FA; Fluka Scientific).

Peptides were then desalted using Oasis HLB 1cc Extraction Cartridges (Waters). Columns were activated by addition of 200 $\mu$ L of HPLC-grade acetonitrile (ACN; Honeywell), followed by four equilibration washes of 100 $\mu$ L 0.1% FA, and a final, fifth equilibration with 100 $\mu$ L of 1% ACN dissolved in 0.1% FA. Peptide samples were then passed through the column, then collected and passed through the column once more. The column was washed three times with 0.1% FA, and then eluted into fresh siliconized tubes through the following washes (expressed as ratios of 0.1% FA:ACN): 100 $\mu$ L of 80:20, 100 $\mu$ L of 50:50, and 2 washes of 100 $\mu$ L of 20:80. The eluted peptides were then concentrated to almost dryness in the speed vacuum, and resuspended in 20 $\mu$ L of 0.1% FA for MS analysis.

#### *2.4.1 NHS-Biotin Labelling and Limited Proteolysis*

For limited proteolysis, 2 plates each of 1 million cells were transfected with 4 $\mu$ g of FLAG-hYVH1 + 7 $\mu$ g of His<sub>6</sub>-Hsp70, or 4 $\mu$ g of FLAG-hYVH1 + 1 $\mu$ g of myc-Src + 6 $\mu$ g of FLAG-EV. The limited proteolysis experiment was carried out as outlined above but was only incubated for 5 minutes at 37°C and was promptly quenched by the addition of 5% FA. The rest of the peptide cleanup was carried out as described.

The NHS-biotinylation protocol utilized the same transfections as the limited proteolysis experiment. After completion of the initial IP washes, all beads were washed twice in PBS and then resuspended in 88 $\mu$ L of PBS. A 20mM stock of EZ-Link NHS-Biotin (Thermo scientific) was prepared fresh in DMSO, and 12 $\mu$ L of this was added to each tube to make up a final volume of 100 $\mu$ L. An incubation was then completed at room temperature for 30 minutes, on a nutator. The biotinylation reaction was then quenched with the addition of 500 $\mu$ L of 0.1M glycine in PBS for 5 min, and then one

more wash in 0.1M glycine, followed by two equilibration washes in 50mM AB before the addition of trypsin and overnight digest.

#### 2.4.2 *hYVH1 Phosphosite Mapping*

Two 15cm plates of 2 million cells were grown out for each sample and were transfected with 10 $\mu$ g of FLAG-hYVH1+2 $\mu$ g of myc-Src, or 10 $\mu$ g of FLAG-hYVH1+2 $\mu$ g FLAG-EV. Plates were administered 1mM of sodium pervanadate, and lysed in lysis buffer that was supplemented with 1mM sodium pervanadate and 1mM NaF. The rest of the protocol was carried out as outlined.

All mass spectrometry experiments were performed on a Waters SYNAPT G2Si quadrupole time of flight mass spectrometer (QTOF-MS) (Waters, Milford, MA). Tryptic peptides were injected and separated on a 1.8  $\mu$ m HSS T3 75  $\mu$ m x 150 mm reverse-phase column (Waters) at a flow rate of 0.3  $\mu$ L/min using a nanoAcquity UPLC autosampler. The peptides were separated by a non-linear gradient consisting of mobile phase A (0.1% FA in water) and mobile phase B (ACN with 0.1% FA). The column was equilibrated using a 97:3 solvent ratio (mobile A:B) and peptides were loaded onto the column at this solvent ratio. Peptide were eluted using a 60 min gradient (3-30% B for 35 min, 30-50% B for 15 min, 85% B for 10 min) and electrosprayed into the QTOF. Electrospray conditions included a 3 kV capillary voltage and a 30 V cone voltage. Calibration was performed using [Glu1]-fibrinopeptide B (50 fmol/ $\mu$ L) in the lock mass channel at m/z 785.8427 for a doubly-charged positive ion. Raw data was collected using Mass Lynx (version 4.1). Putative phosphopeptides were reanalyzed by selected-ion reaction monitoring (SRM) whereby the parent ion mass of interest was selected in the quadrupole and fragmented in the transfer following ion mobility separation. The TOF

pusher frequency was synchronized to enhance sensitivity of fragmentation. Phosphorylation site mapping was assigned by manual analysis of the fragment pattern. Progenesis software was used for protein identification and quantitation.

For Hsp70 association experiments (both for quantitating Src effect, and Y35E mutant), hYVH1 and Hsp70 abundance intensity data was normalized to the top three peptides present in each sample via Progenesis. Samples were then normalized to the amount of hYVH1 present to assess differences in Hsp70, then expressed as ratios relative to one. For limited trypsin digestion and NHS-Biotin labeling experiments, tryptic peptide intensity measurements were normalized to levels acquired in the hYVH1 minus Hsp70 samples. These values were expressed as ratios relative to one to assess fold-change, using a high confidence peptide that remained unchanged in abundance between samples as the normalized value. Mean values between replicates were plotted on the graphs. Statistical significance was determined using a two-tailed student's T-test on a 95% confidence interval, or a 99% confidence interval (where indicated).

## 2.5 SDS-PAGE and Western Blotting

Affinity chromatography beads used for western blot analysis were resuspended in 40 $\mu$ L of 6X SDS loading buffer, and cellular lysates were administered loading buffer in a 5:1, lysate:buffer ratio. Both samples were denatured at 95°C for 5 minutes prior to SDS-PAGE. SDS-PAGE gels were produced for western blots, with the endogenous experiments run on 10% gels for 1.5 hours at 125V, and all others run on 12% gels for 2 hours at 125V. Gel proteins were transferred onto polyvinylidene difluoride (PVDF) membranes at 100V for 1 hour, which were then blocked in 5% skim milk or bovine serum albumin (BSA) in 1X TBST. Membranes were then incubated at 4°C overnight on a rocker with one of the following antibodies (Table 2.1), mixed in 2.5% skim milk or BSA.

Antibody	Source	Concentration Used
Mouse monoclonal anti-FLAG M2	Sigma	1:4000
Mouse monoclonal anti-His	Santa Cruz	1:2000
Mouse monoclonal anti-Myc	Santa Cruz	1:1000
Mouse anti-phosphotyrosine, clone 4G10	Millipore	1:4000
Mouse anti-phosphotyrosine	Cell Signalling	1:2000
Rabbit anti-hYVH1	Dixon Lab*	1:4000
Rabbit anti-actin	Sigma	1:4000
Rabbit anti-Src	Cell Signalling	1:2000
Rabbit anti-Hsp70	Cell Signalling	1:2000

**Table 2.1 List of primary antibodies used for western blots.** A list of antibodies used to probe for proteins of interest, complete with their commercial source and the optimal concentration that they were used in. The rabbit anti-hYVH1 is not a commercial antibody that is available for purchase.

Blots were then washed three times in 1X TBST, before a 45-minute room temperature incubation with either goat anti-mouse (1:2000; Sigma) or goat anti-rabbit (1:2000; BioRad) secondary antibody, on a rocking platform. Streptavidin conjugated with horseradish peroxidase (Strep-HRP; 1:2000; Pierce) was used in place of both a primary and secondary antibody when probing for biotin integration. Blots were then washed three times more with TBST before imaging on a BioRad ChemiDoc imager with the SuperSignal West Femto Maximum Sensitivity Substrate chemiluminescent imaging kit (Thermo scientific). Densitometry analysis was performed using ImageJ software (NIH).

## **CHAPTER 3: RESULTS AND DISCUSSION**

### **3.1 Endogenous Phosphorylation of hYVH1 by Src**

#### *3.1.1 Rationale for Examining Endogenous Phosphorylation*

Recently, our lab reported that cells co-expressing hYVH1 and Src display increased translational activity, in which evidence was provided to suggest Src phosphorylation of hYVH1 results in alterations of the 80S proteome that promotes increased translational fidelity.<sup>51</sup> This study was the first paper published that has implicated hYVH1 as a novel substrate of Src kinase, and proposed that Src phosphorylation of the linker region of hYVH1 at Tyr179 induces localization to the nucleus – presumably to expedite the nuclear shuttling of translationally fit 60S ribosomal subunits. Most of the investigation into ribosome biogenesis has been performed thus far through yeast models.<sup>62</sup> In contrast, this recent publication attempted to elucidate the impact of hYVH1 on the ribosome through a human cell model (HeLa cells). In this endeavour, several experiments were performed to observe changes at the ribosome level in response to protein overexpression using phosphotyrosine immunoblotting as a readout. In order to complement these overexpression studies, we were interested in confirming the phosphorylation using alkaline phosphatase treatment followed by exploring the phosphorylation of hYVH1 by Src at the endogenous level.

#### *3.1.2 Src Kinase Phosphorylates hYVH1*

Initial studies did identify endogenous Src in an hYVH1 interactome, followed by the phosphorylation of hYVH1 by Src being reproducibly observed by our lab.<sup>60</sup> To

confirm the immunoblotting results, an alkaline phosphatase treatment was performed on samples co-expressing FLAG-hYVH1 and Myc-Src Y530F (**Figure 3.1A**). The results showed that the sample subjected to alkaline phosphatase treatment displayed significantly lower phosphotyrosine signal, which supports the authenticity of the phosphorylation event and rules out off-target antibody reactions. The change in signal was quantified by densitometry analysis (**Figure 3.1B**); phosphotyrosine band intensity was normalized to account for potential inequalities in the amount of hYVH1 and Src present in each sample. The results show that Src phosphorylates hYVH1, and the signal is adequately diminished upon introducing an alkaline phosphatase. The decrease in phosphorylation due to phosphatase treatment was not statistically significant, although was consistently reproducible, and at minimum, shows a 1.5-fold reduction in phosphorylation. These results corroborate previous findings that Src can phosphorylate hYVH1 in an overexpressed model.

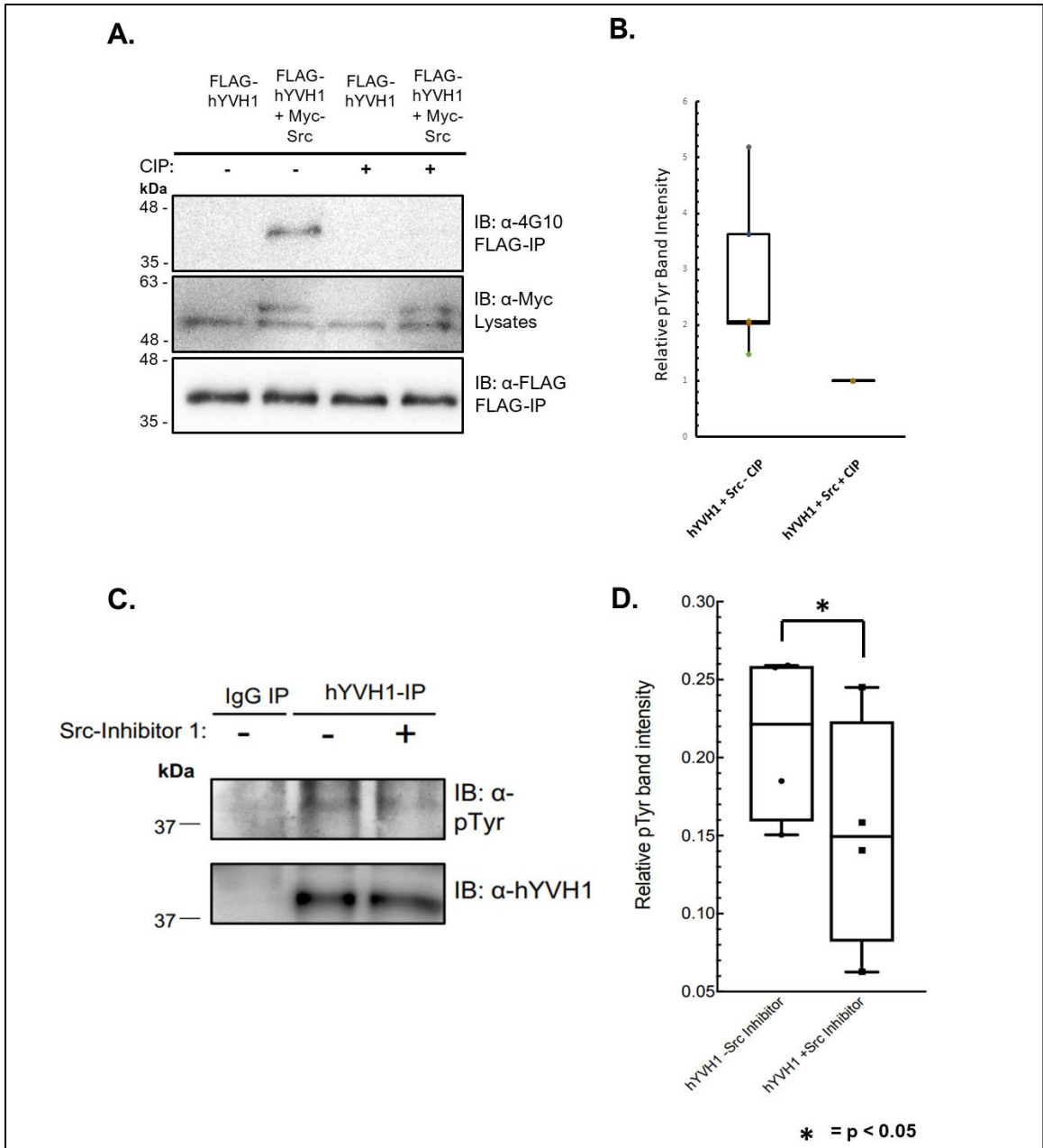


**Figure 3.1. Phosphorylation of hYVH1 by Src in both an overexpressed and endogenous model.** A) A demonstration of hYVH1 phosphorylation by Src using HeLa samples overexpressing FLAG-hYVH1, or FLAG-hYVH1 and Myc-Src. The two lanes on the right have been treated with alkaline phosphatase. The top panel shows Tyr phosphorylation on a FLAG-IP, the middle panel shows the presence of Src in the cellular lysates, and the bottom panel verifies the amount of FLAG-hYVH1 in each lane. B) ImageJ-obtained densitometry measurements of 4G10 blots for the two Src-transfected lanes. Normalized to the amount of FLAG-hYVH1 and Myc-Src present in each sample (n=5). C) Endogenous hYVH1 phosphorylation by Src in HeLa cells. The left lane is a rabbit serum control for the anti-hYVH1 IP. The centre lane is treated with

DMSO, and the right lane is treated with SI-1. The top panel is a blot for tyrosine phosphorylation of an hYVH1-IP, and the bottom panel is a blot for hYVH1 in an hYVH1-IP. **D)** ImageJ-obtained densitometry measurements of 4G10 blots for the two experimental lanes. Normalized to the amount of hYVH1 present in each sample (n=4).

### *3.1.3 Endogenous Phosphorylation of hYVH1 by Src*

Although the Src Y530F mutant used is constitutively active, it is a well-documented oncogenic mutation that is disease relevant.<sup>59</sup> To verify that Src phosphorylation of hYVH1 is physiologically consistent under basal conditions, attempts were made to pull down endogenous hYVH1 from HeLa cells and assess tyrosine phosphorylation in response to a Src inhibitor. The method developed to assess this involved a serum starvation, followed by the addition of FBS-fortified media, pervanadate, Src-Inhibitor 1 (SI-1), and epidermal growth factor (EGF) to cells in culture to increase basal tyrosine phosphorylation to a detectable threshold. Serum starvation was performed to synchronize cells and to exaggerate the effects of growth factor induced Src activation from the re-addition of FBS.<sup>66</sup> Sodium orthovanadate ( $\text{Na}_3\text{VO}_4$ ) is a reversible PTP inhibitor and acts as a phosphate analogue – binding to the catalytic Cys instead of a phosphate moiety.<sup>67</sup> This treatment allows for the capture of transient phosphorylation states, especially fleeting ones, as PTP inhibition traps phosphates on the Tyr residues of their protein substrates. Orthovanadate can be complexed with  $\text{H}_2\text{O}_2$  to produce pervanadate, which further inhibits PTPs by binding and irreversibly oxidizing the thiol group of catalytic cysteines of PTPs into sulfonic acid.<sup>68</sup> Epidermal growth factor (EGF) was added to further stimulate Tyr phosphorylation by activating Src through the EGFR signal cascade.<sup>69,70</sup> The difference in endogenous Tyr phosphorylation provided by Src

activity was visualized by inhibiting Src with SI-1, which operates by competitively binding to the enzyme's ATP-binding and peptide-binding regions.<sup>71</sup>

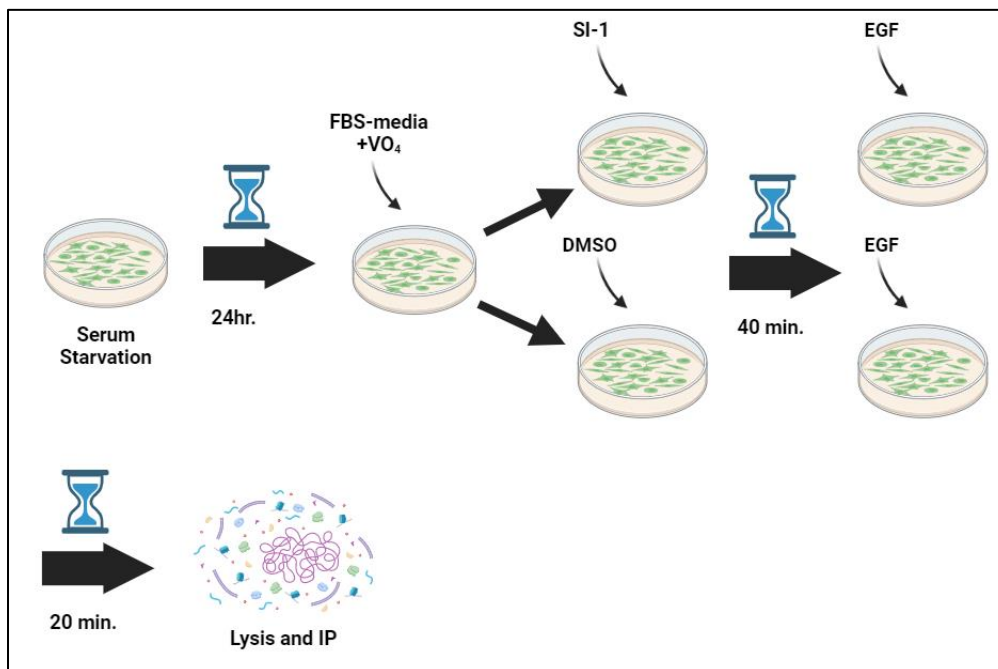


**Figure 3.2. Workflow for determining the endogenous phosphorylation of hYVH1 by Src kinase.** HeLa cells were serum starved for 24 hours, then incubated with fresh FBS and pervanadate to stimulate tyrosine phosphorylation by Src and inhibit PTP activity. Plates were administered either the SI-1 Src inhibitor, or DMSO at this time. After 40 minutes, they were treated with EGF for 20 minutes to trigger growth-factor induced Src activation, then lysed and immunoprecipitated with a rabbit anti-hYVH1 antibody that was prebound to a Protein A agarose resin. Figure produced in BioRender.

In response to the addition of SI-1, results indicated a statistically significant decrease in tyrosine phosphorylation in endogenous hYVH1 (**Figure 3.1C, D**). While there is an observed decrease, the low level of endogenous phosphorylated hYVH1 detected indicates that the stoichiometry of phosphorylation may not be optimal. This suggests that the HeLa cell may be a poor cellular model for Src-mediated hYVH1 phosphorylation, and other cell models that display higher Src activity should be explored

in the future. Another consideration may be the physiological context in which this phosphorylation event occurs. One potential condition would be oxidative stress, which may lead to increased Src phosphorylation of hYVH1 as Src has been shown to be activated by oxidative stress.<sup>72</sup>

In retrospect, an additional cause for low phosphorylation levels may be the inhibition of all PTPs by pervanadate. Src activity is increased by dephosphorylation of Tyr530, an action performed by PTPs such as SHP-2 and PTP-1B.<sup>73</sup> This mechanism is irrelevant when using a constitutively active Src Y530F mutant, as one can safely use orthovanadate to enrich for Src-induced phosphorylation without concern for deactivating the enzyme. However, wild-type Src would be rendered inactive by the potential inhibition of its PTP activators. Furthermore, with hYVH1 being a PTP itself, this experiment also operates on the predicate assumption that pervanadate-mediated inhibition of the catalytic domain of hYVH1 (or oxidation of any of its C-terminal cysteines) does not alter its conformation to one less amenable to Src phosphorylation. Future attempts with more targeted PTP inhibition may be possible once the phosphatases that act on hYVH1 are identified.

With these limitations accounted for, these results provide preliminary evidence of endogenous phosphorylation of hYVH1 by Src kinase. However, further experimentation and optimization is required to increase the resolution and consistency of this observation.

### 3.2 Quantifying the hYVH1-Hsp70 Complex Dissociation by Src

In addition to a proteome-altering effect at the ribosome, Src co-expression with hYVH1 also potentially abrogates the hYVH1-Hsp70 complex.<sup>60</sup> hYVH1 and Hsp70 were formerly observed by our lab to associate together through both *in vitro* and *in vivo* co-IP experiments,<sup>43</sup> and both display tyrosine phosphorylation by Src – which implies that this interaction is regulated by phosphorylation.<sup>60</sup> Since Hsp70 is also present at the ribosome and the hYVH1-Hsp70 complex has been shown to increase cell survival,<sup>43</sup> it is critical to understand the mechanistic details of hYVH1-Hsp70 complex formation, how Src acts upon it, and what role this interaction might play in the contexts of ribosome biogenesis and cell survival.

Although we have previously examined the hYVH1-Hsp70 interaction by immunoblotting experiments,<sup>60</sup> we were interested in examining the complex dissociation mediated by Src using label-free quantitative mass spectrometry. This was performed by transfecting FLAG-hYVH1 in the presence and absence of Src and isolating the hYVH1-Hsp70 complex by FLAG immunoprecipitation using magnetic beads. Proteins were prepared for mass spectrometry by trypsin digestion directly off the magnetic beads followed by sample cleanup. Peptides were subjected to data-independent acquisition mass spectrometry and quantitated by label free MS1 peptide intensity measurement. Following peptide identification, intensity values were then normalized across both samples to express endogenous Hsp70 pulldown efficiency as a function of hYVH1 quantity (**Figure 3.3**).

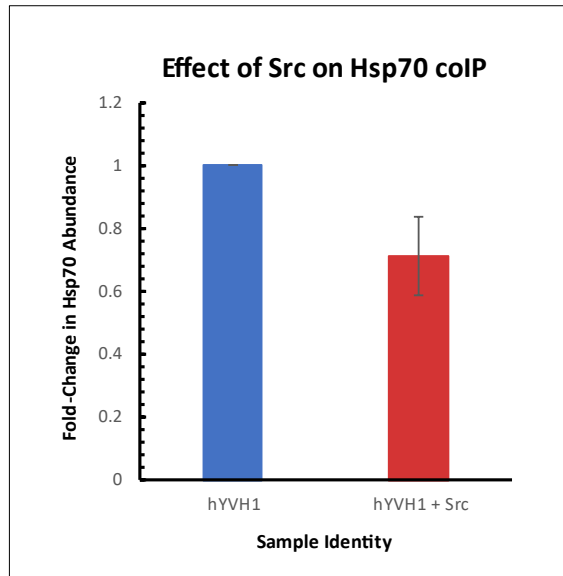


**Figure 3.3. Quantitation of Src’s effect on hYVH1’s ability to coIP Hsp70.** A bar graph of aggregated MS data, highlighting the difference in endogenous Hsp70 coIP efficiency in the presence of Src. All hYVH1 and Hsp70 peptides were normalized to the top three most abundant peptides in each sample, and then normalized to the amount of hYVH1 between all trials and samples (n=3). All trials were then normalized to the -Src sample, and the averages are expressed.

From **Figure 3.3**, we can see that there was an observed 29% decrease in Hsp70 coprecipitation by hYVH1 in the presence of Src. This finding was not statistically significant, indicating that the variability between samples was too wide to conclude the exact magnitude of Src’s effect. Nevertheless, this trend is consistent with past observations by our lab and demonstrates that Src expression attenuates the hYVH1-Hsp70 complex. These results also demonstrate the utility of label-free quantitative mass spectrometry for the examination of protein-protein interaction dynamics.

### **3.3 The hYVH1-Hsp70 binding interface**

#### *3.3.1 Rationale for Binding Site Identification*

Our lab has previously studied the hYVH1-Hsp70 complex using domain-deleted variants in co-IP experiments to determine the structures necessary for these two proteins to interact.<sup>43</sup> Identifying the molecular determinants of this interaction would allow for the creation of binding site variants that may act as dominant-positive and dominant-negative mutants. These mutants could serve as excellent tools to provide insight into the cellular function of the hYVH1-Hsp70 complex. It was previously shown that the hYVH1-Hsp70 complex could be maintained exclusively by the ATPase domain of Hsp70. However, neither the isolated DUSP domain nor the zinc-binding domain (ZBD) of hYVH1 could conclusively co-precipitate Hsp70, which led to the conservative conclusion that both domains of hYVH1 contributed to binding to Hsp70.<sup>43</sup> Furthermore, these domain deletion methods could not provide sufficient detail to identify the exact protein surfaces where the association occurs. We were therefore interested in utilizing structural mass spectrometry approaches to examine the binding mechanism using full-length proteins.

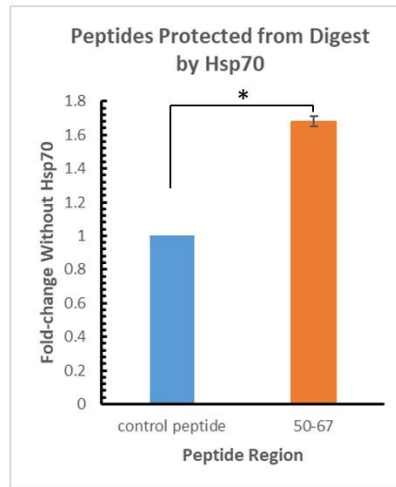
#### *3.3.2 In-Solution Limited Proteolysis*

The first MS method to determine the binding interface was an in-solution, limited proteolysis. HeLa cultures were transfected with either hYVH1 and Src, or hYVH1 and Hsp70, lysed, and then subjected to FLAG co-IP to pull down hYVH1 and any bound Hsp70. Instead of standard overnight digestion, co-IPs were subjected to a brief, 5-minute tryptic digest that was promptly quenched by adding formic acid. This narrow time frame is the main principle of limited proteolysis, which operates under the

assumption that only the most solvent-accessible cleavage sites would be cut by the enzyme during this short duration.<sup>74</sup> The resulting MS spectrum only represents a fraction of the total possible peptides. However, this output allows for inferences about the steric accessibility of the peptides that are either absent or detected. The co-transfection of hYVH1 with Src was another deliberate decision, as the ability of Src to disrupt the hYVH1-Hsp70 complex could be leveraged to decrease the amount of endogenous Hsp70 pulled down in the control sample by hYVH1. By resolving MS1 intensity measurements between hYVH1-transfected samples to samples co-expressing hYVH1 and Hsp70, we can determine regions of the protein that are presumably shielded from digestion by Hsp70.

Preliminary attempts at this experiment by others had implicated three peptide regions on hYVH1 that were protected from digestion in the presence of Hsp70, corresponding to amino acid positions: 68-77, 141-153, and 154-163.<sup>60</sup> While this result was promising, the preliminary efforts used manual comparison of peptide intensity rather than rigorous normalization using mass spectrometry processing software. Moreover, the experimental design did not account for the abundance of cysteine residues in hYVH1 and thus suffered from low sequence coverage, particularly in the C-terminal ZBD containing 7 cysteine residues. To achieve better sequence coverage, samples were reduced with DTT and alkylated with iodoacetamide before mass spectrometry analysis to prevent the spontaneous reformation of non-specific disulfides between the thiol groups of cysteine residues and thus allow for the measurement of cysteine-containing peptides.

A.



B.

10	20	30	40	50	60
MLEAPGPSDG	CELSNPSASR	VSCAGQMLEV	QPGLYFGGAA	AVAEPDHLRE	AGITAVLTVD
70	80	90	100	110	120
SEEPSFKAGP	GVEDLWRLFV	PALDKPETDL	LSHLDRCVAF	IGQARAEGRA	VLVHCHAGVS
130	140	150	160	170	180
RSVAIITAFI	MKTDQLPFEK	AYEKLQILKP	EAKMNEGFEE	QLKLYQAMGY	EVDTSIAIYK
190	200	210	220	230	240
QYRLQKVTEK	YPELQNLPEE	LFAVDPTTVS	QGLKDEVLYK	CRKCRSLFR	SSSILDHREG
250	260	270	280	290	300
SGPIAFAHKR	MTPSSMLTTG	RQAQCTSYFI	EPVQWMSAL	LGVMDGQLLC	PKCSAKLGSE
	310	320	330	340	
	NWYGEQCSCG	RWITPAFQIH	KNRVDEMKIL	PVLGSQTGKI	

59.7% sequence coverage

C.

**Peptide retention time, identification scores, and neutral masses**

Retention Time (min)	Neutral mass	Best identification Score	Sequence	Modifications	Max fold change	Highest mean condition
23.542	1098.549	7.268	AGPGVEDLWR		0.93	hYVH1 & Hsp70
<b>29.883</b>	<b>1891.945</b>	<b>7.246</b>	<b>EAGITAVLTVDSEEPSFK</b>		<b>1.72</b>	<b>hYVH1</b>
13.561	1268.697	6.826	EGSGPIAFAHKR		1.19	hYVH1
36.163	2178.200	6.981	LFVPALDKPETDLLSHLDR		1.21	hYVH1
14.536	1038.689	7.172	LQILKPEAK		1.23	hYVH1
23.944	1937.911	7.898	LYQAMGYEVDTSIAIK		1.04	hYVH1
24.620	2385.099	7.690	LYQAMGYEVDTSIAIKQYR		1.10	hYVH1
20.595	2401.098	7.690	LYQAMGYEVDTSIAIKQYR	[5] Oxidation M	1.23	hYVH1
26.346	1280.577	7.474	MNEGFWEQLK		1.20	hYVH1
16.262	1180.557	6.877	MTPSSMLTTGR		1.21	hYVH1
42.406	1192.686	7.211	SVAIITAFLMK		0.97	hYVH1 & Hsp70
16.774	976.497	7.349	TDQLPFEK		1.09	hYVH1
25.186	1239.713	6.435	WITPAFQIHK		1.00	hYVH1 & Hsp70

**Peptide normalized abundances across 3 trials**

Sequence	Modifications	Max fold change	Highest mean condition	Normalized abundance					
				hYVH1			hYVH1 + Hsp70		
				Trial 1	Trial 2	Trial 3	Trial 1	Trial 2	Trial 3
AGPGVEDLWR		0.93	hYVH1 & Hsp70	302236.8	277835.5	664123.8	355373.1	372033.6	712233.5
<b>EAGITAVLTVDSEEPSFK</b>		<b>1.72</b>	<b>hYVH1</b>	<b>14155.6</b>	<b>86773.6</b>	<b>95757.0</b>	<b>8223.8</b>	<b>51658.0</b>	<b>58333.4</b>
EGSGPIAFAHKR		1.19	hYVH1	8846.3	4469.6	1998.1	12089.4	4226.5	1683.4
LFVPALDKPETDLLSHLDR		1.21	hYVH1	153706.1	12541.0	797.8	141499.9	10387.9	844.1
LQILKPEAK		1.23	hYVH1	122337.0	36304.4	36195.5	129568.6	29451.2	30534.4
LYQAMGYEVDTSIAIK		1.04	hYVH1	25603.2	58792.9	86792.2	24505.3	57084.6	89346.5
LYQAMGYEVDTSIAIKQYR		1.10	hYVH1	71458.2	121180.3	106821.4	64770.8	119666.3	143064.0
LYQAMGYEVDTSIAIKQYR	[5] Oxidation M	1.23	hYVH1	46226.5	53462.8	102939.3	38368.7	54882.2	83529.4
MNEGFWEQLK		1.20	hYVH1	106829.8	272892.9	406273.0	101966.3	238913.4	337994.4
MTPSSMLTTGR		1.21	hYVH1	697352.6	375930.4	28850.9	574583.6	340173.2	30084.1
SVAIITAFLMK		0.97	hYVH1 & Hsp70	39565.1	73436.3	65247.9	55241.4	75506.2	81498.7
TDQLPFEK		1.09	hYVH1	55980.5	69184.1	7992.8	67695.5	76027.2	7312.9
WITPAFQIHK		1.00	hYVH1 & Hsp70	11313.4	3572.1	5290.2	19373.8	4146.4	5316.2

**Figure 3.4. Results of the limited digest of hYVH1.** **A)** A bar graph displaying the significant differentially encountered peptides (n=3), relative to a control peptide that remained unchanged in abundance between samples after normalization. The identified peptides were all considered for normalization to acquire a correction factor to apply using the Progenesis software. Peptides reproducibly above a 1.5-fold change were considered significant. **B)** The amino acid sequence of hYVH1, illustrating the peptides identified by limited digestion in red and blue (coloured to show peptide boundaries). Sequence coverage is expressed as a percentage at the bottom. **C)** Tables showing significant peptides identified from all three trials of limited in-solution trypsin proteolysis. The peptide corresponding to amino acids 50-67 is highlighted in red.

As shown in **Figure 3.4A**, a peptide corresponding to position 50-67 remained protected by Hsp70 co-expression and was detected at a much lower level in all three biological replicates (**Figure 3.4B**). This region exists just upstream of the previously reported 68-77 region, indicating that a region around Lys 67 may be critical in mediating the interaction with Hsp70. None of the formerly identified peptides were reproduced; however, it is noteworthy that the acquired 59.7% sequence coverage of hYVH1 is higher than previously reported by others (**Figure 3.4B**). This shift in identified peptides may be the consequence of more complete tryptic digestion. Interestingly, despite including an alkylation step, the Cys-containing peptides in hYVH1 were still present in much lower abundance, suggesting that they are providing structural stabilization in a more interior region of the protein.

One important consideration of the limited tryptic digestion approach is that the resolution of binding interfaces is inherently restricted by the boundaries of tryptic cut sites. Identification of these solvent-shielded regions is dependent on the spatial arrangement of a handful of lysine and arginine residues.<sup>12</sup> Despite this constraint, the data supports our earlier hypothesis of an Hsp70 binding interface in the N-terminus, specifically in proximity to amino acids 50-67 on hYVH1.

### *3.3.3 NHS-biotin Labelling to Determine Binding Interface*

To complement the results provided by limited proteolysis, we employed a differential biotin labelling approach coupled with mass spectrometry that allowed us to examine the hYVH1-Hsp70 interaction using full digestion protocol. In this method, the hYVH1-Hsp70 complex was isolated as described for the limited proteolysis experiment. This IP was then followed by a 30-minute room temperature incubation in NHS-biotin,

which was quenched afterwards with a glycine-fortified PBS wash to react with and remove the excess biotin from the sample. NHS-biotin is a pre-activated form of biotin that can covalently react with free amide groups, including the N-termini of polypeptides and the side chains of lysine residues, without the need for a biotin ligase enzyme. This makes it an effective tool to biotinylate proteins *in vitro* without introducing enzymatic contaminants.<sup>75</sup> The biotinylated proteins were subjected to an overnight on-bead trypsin digest before reduction and alkylation, Oasis cleanup, and MS analysis (**Figure 3.5**).

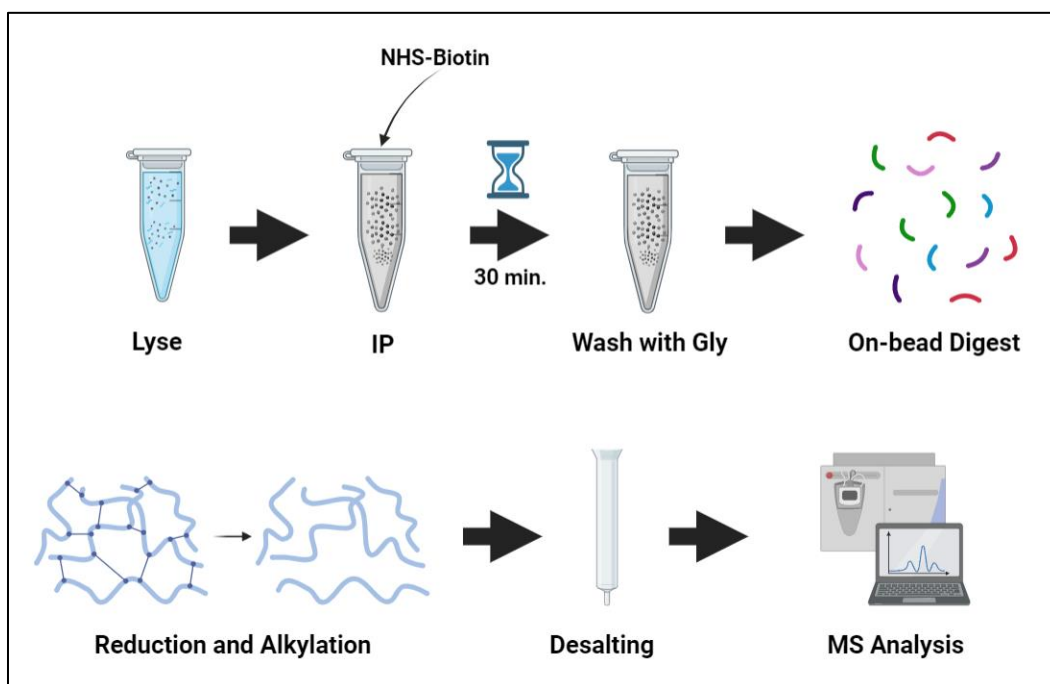
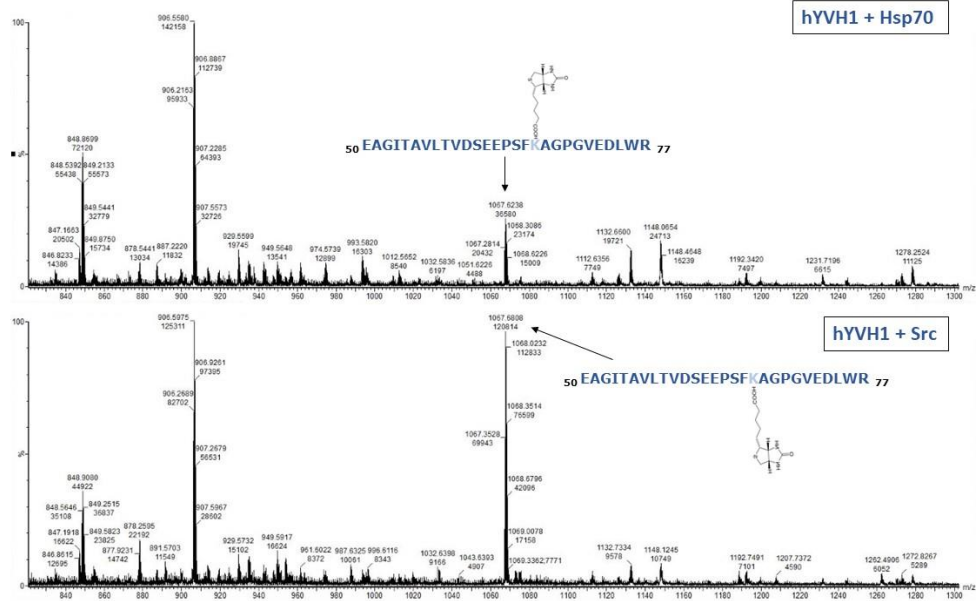


**Figure 3.5. Workflow to determine the binding interface via NHS-biotinylation.** Transfected samples were lysed and then subjected to anti-FLAG IP. NHS-biotin was added to the washed resin and incubated for 30 minutes, followed by washing in glycine. These samples were then digested in solution with trypsin, subjected to thiol reduction and alkylation, and desalted with an Oasis column before MS analysis. Figure produced in BioRender.

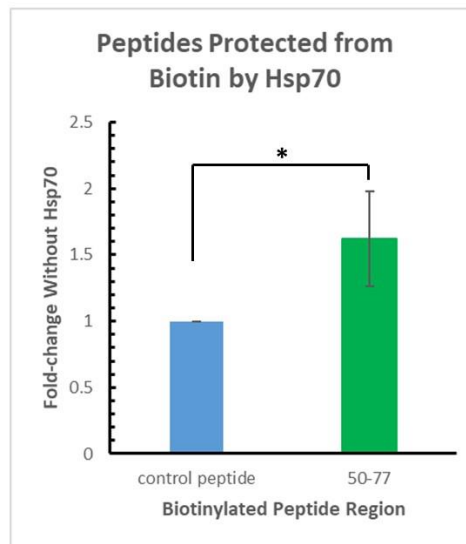
Theoretically, this would allow for biotin integration on all lysine-containing peptides that are solvent-exposed and accessible to biotin. The resultant biotinylated lysine residues would be resistant to trypsin cleavage, as the chemical group interferes

with the enzyme's ability to cleave C-terminal to lysine (although arginine residues will remain unaffected).<sup>75</sup> The rationale behind this experiment is that solvent-exposed lysine residues may be present on the binding interface between two proteins, possibly contributing to electrostatic interactions between the surfaces. hYVH1 samples that co-expressed Hsp70 would then possess an occupied surface that is now rendered inaccessible to biotin and is, therefore, now available for trypsin cleavage.<sup>75</sup> On an MS spectrum, it would be expected that a peptide region that is not interacting with Hsp70 would possess a biotinylated Lys (and an upshift in mass, corresponding to 226.3 Da) in both the presence and absence of Hsp70, with a missed cleavage at that Lys residue. On the other hand, lysine-containing peptide regions that *are* interacting with Hsp70 will display lower levels of biotinylation and will be present in less abundance when Hsp70 is present.

A.



B.



\* =  $p < 0.05$

C.

### Peptide retention time, identification scores, and neutral masses

Retention Time (min)	Neutral mass	Best identification Score	Sequence	Modifications	Max fold change	Highest mean condition
35.198	1982.035	6.8518	AYEKLQILKPEAK	[4] Biotin K [9] Biotin K	2.73	hYVH1
31.234	2491.994	6.0991	CSAKLGSFNWYGEQCSCGR	[1] Carbamidomethyl C [4] Biotin K [15] Carbamidomethyl C [17] Carbamidomethyl C	2.30	hYVH1
45.725	3199.562	6.2331	EAGITAVLTVDSSEPSFKAGPVEDLWR	[18] Biotin K	3.44	hYVH1
46.956	2673.284	6.9036	EGSGPIAFAHKRMTTPSSMLTTGR	[11] Biotin K [18] Oxidation M	1.64	hYVH1
47.037	2673.309	6.9036	EGSGPIAFAHKRMTTPSSMLTTGR	[11] Biotin K [18] Oxidation M	1.37	hYVH1
44.705	2673.317	6.5212	EGSGPIAFAHKRMTTPSSMLTTGR	[11] Biotin K [18] Oxidation M	1.03	hYVH1 + Hsp70
44.705	2673.213	6.5212	EGSGPIAFAHKRMTTPSSMLTTGR	[11] Biotin K [18] Oxidation M	1.05	hYVH1 + Hsp70
42.774	2689.244	6.4023	EGSGPIAFAHKRMTTPSSMLTTGR	[11] Biotin K [13] Oxidation M [18] Oxidation M	1.63	hYVH1
36.224	1450.825	8.32	ILPVLGSQTGKI	[11] Biotin K	2.29	hYVH1
43.715	2404.241	8.3474	LFVLPALDKPETDLLSHLDR	[8] Biotin K	2.18	hYVH1
41.512	2769.326	7.2143	LQILKPEAKMNEGFWEQQLK	[5] Biotin K [9] Biotin K [10] Oxidation M	2.44	hYVH1
37.569	2527.214	6.2829	LQILKPEAKMNEGFWEQQLK	[5] Biotin K	1.86	hYVH1
27.424	2627.153	6.6091	LYQAMGYEVDTSAYIKQYR	[5] Oxidation M [17] Biotin K	2.21	hYVH1
31.244	2611.191	6.9614	LYQAMGYEVDTSAYIKQYR	[17] Biotin K	2.10	hYVH1
41.696	2611.213	6.2544	LYQAMGYEVDTSAYIKQYR	[17] Biotin K	1.14	hYVH1 + Hsp70
27.076	2226.135	7.5895	NRVDEMKILPVLGSQTGKI	[6] Oxidation M [7] Biotin K	1.62	hYVH1
43.828	2549.260	7.6967	NRVDEMKILPVLGSQTGKI	[7] Biotin K [18] Biotin K	2.24	hYVH1
39.428	2565.255	7.5403	NRVDEMKILPVLGSQTGKI	[6] Oxidation M [7] Biotin K [18] Biotin K	2.07	hYVH1
40.127	2565.241	6.1758	NRVDEMKILPVLGSQTGKI	[6] Oxidation M [7] Biotin K [18] Biotin K	2.11	hYVH1
32.466	2603.295	6.5616	SVAIITAFMLKTDQLPFEKAYEK	[11] Biotin K [19] Biotin K	1.52	hYVH1 + Hsp70
42.889	3094.495	6.5315	SVAIITAFMLKTDQLPFEKAYEK	[19] Biotin K [23] Biotin K	1.32	hYVH1 + Hsp70
28.461	1919.973	6.2909	TDQLPFEKAYEK	[8] Biotin K [12] Biotin K	1.26	hYVH1 + Hsp70
26.807	1693.819	7.8293	TDQLPFEKAYEK	[8] Biotin K	3.16	hYVH1
35.331	1940.013	6.2676	VDEMKILPVLGSQTGKI	[5] Biotin K	2.33	hYVH1
31.695	1940.033	5.7813	VDEMKILPVLGSQTGKI	[5] Biotin K	1.35	hYVH1 + Hsp70
29.951	1955.996	6.5241	VDEMKILPVLGSQTGKI	[4] Oxidation M [5] Biotin K	1.38	hYVH1
47.590	2279.153	8.7089	VDEMKILPVLGSQTGKI	[5] Biotin K [16] Biotin K	2.18	hYVH1
42.723	2295.143	8.4368	VDEMKILPVLGSQTGKI	[4] Oxidation M [5] Biotin K [16] Biotin K	2.12	hYVH1
36.893	1465.761	7.0274	WITPAFQIHK	[10] Biotin K	2.39	hYVH1
49.275	3975.891	6.8159	YPELQNLQELFAVDPTTVSQGLKDEVLYKCR	[30] Biotin K [31] Carbamidomethyl C	4.37	hYVH1

### Peptide normalized abundances across 3 trials

Sequence	Modifications	Max fold change	Highest mean condition	Normalized abundance					
				hYVH1 Trial 1	hYVH1 Trial 2	hYVH1 Trial 3	hYVH1 + Hsp70 Trial 1	hYVH1 + Hsp70 Trial 2	hYVH1 + Hsp70 Trial 3
AYEKLQILKPEAK	[4] Biotin K [9] Biotin K	2.73	hYVH1	42333.0	91967.0	102514.4	30364.9	28398.2	28035.8
CSAKLGSFNWYGEQCSCGR	[1] Carbamidomethyl C [4] Biotin K [15] Carbamidomethyl C [17] Carbamidomethyl C	2.30	hYVH1	4510.2	10791.2	13352.9	3517.1	4285.4	4675.9
EAGITAVLTVDSSEPSFKAGPVEDLWR	[18] Biotin K	3.44	hYVH1	871174.9	605158.7	476711.1	285481.3	176983.7	105916.6
EGSGPIAFAHKRMTTPSSMLTTGR	[11] Biotin K [18] Oxidation M	1.64	hYVH1	39953.5	16284.8	15062.2	25011.7	9768.9	8778.6
EGSGPIAFAHKRMTTPSSMLTTGR	[11] Biotin K [18] Oxidation M	1.37	hYVH1	1314.5	487.0	382.1	729.2	441.1	419.7
EGSGPIAFAHKRMTTPSSMLTTGR	[11] Biotin K [18] Oxidation M	1.03	hYVH1 + Hsp70	10207.7	10362.8	15540.7	14813.8	11478.8	10957.4
EGSGPIAFAHKRMTTPSSMLTTGR	[11] Biotin K [18] Oxidation M	1.05	hYVH1 + Hsp70	36.4	489.4	751.7	303.1	444.0	597.8
EGSGPIAFAHKRMTTPSSMLTTGR	[11] Biotin K [13] Oxidation M [18] Oxidation M	1.63	hYVH1	7754.0	3406.5	3469.8	4948.2	1903.4	2138.4
ILPVLGSQTGKI	[11] Biotin K	2.29	hYVH1	465862.4	650130.9	604628.9	332321.6	208027.3	211122.9
LFVLPALDKPETDLLSHLDR	[8] Biotin K	2.18	hYVH1	3154276.9	3170846.6	3181220.9	2034503.5	1158993.1	1160188.0
LQILKPEAKMNEGFWEQQLK	[5] Biotin K [9] Biotin K [10] Oxidation M	2.44	hYVH1	4100.2	12480.6	14787.8	4609.1	4313.9	3950.3
LQILKPEAKMNEGFWEQQLK	[5] Biotin K	1.86	hYVH1	10974.7	15144.6	16766.7	5869.8	8191.3	8990.5
LYQAMGYEVDTSAYIKQYR	[5] Oxidation M [17] Biotin K	2.21	hYVH1	12198.0	22349.6	26054.8	9521.5	8842.8	9027.8
LYQAMGYEVDTSAYIKQYR	[17] Biotin K	2.10	hYVH1	13005.1	14640.4	18134.7	4888.2	8411.2	8516.0
LYQAMGYEVDTSAYIKQYR	[17] Biotin K	1.14	hYVH1 + Hsp70	4011.0	3199.9	3735.6	6108.5	3064.8	3261.1
NRVDEMKILPVLGSQTGKI	[6] Oxidation M [7] Biotin K	1.62	hYVH1	18555.7	34794.4	32161.7	20918.6	15434.9	16375.8
NRVDEMKILPVLGSQTGKI	[7] Biotin K [18] Biotin K	2.24	hYVH1	67374.7	123967.8	115385.2	54657.2	42332.6	39807.2
NRVDEMKILPVLGSQTGKI	[6] Oxidation M [7] Biotin K [18] Biotin K	2.07	hYVH1	30221.2	61628.1	61529.9	21079.2	26395.8	26475.4
NRVDEMKILPVLGSQTGKI	[6] Oxidation M [7] Biotin K [18] Biotin K	2.11	hYVH1	25582.2	23031.9	25536.4	14967.8	10004.7	10115.9
SVAIITAFMLKTDQLPFEKAYEK	[11] Biotin K [19] Biotin K	1.52	hYVH1 + Hsp70	2132.4	1381.8	1568.7	2536.9	2563.8	2627.8
SVAIITAFMLKTDQLPFEKAYEK	[19] Biotin K [23] Biotin K	1.32	hYVH1 + Hsp70	15989.9	18894.0	20126.1	35155.2	19003.4	18573.6
TDQLPFEKAYEK	[8] Biotin K [12] Biotin K	1.26	hYVH1 + Hsp70	64709.4	46973.3	48733.7	95411.7	54233.6	52459.3
TDQLPFEKAYEK	[8] Biotin K	3.16	hYVH1	44945.6	194056.7	186499.7	44212.1	46627.3	43960.2
VDEMKILPVLGSQTGKI	[5] Biotin K	2.33	hYVH1	39001.1	74788.3	79345.8	30758.9	26190.4	25889.2
VDEMKILPVLGSQTGKI	[5] Biotin K	1.35	hYVH1 + Hsp70	17951.9	11589.3	11080.5	29519.8	12937.5	12937.5
VDEMKILPVLGSQTGKI	[4] Oxidation M [5] Biotin K	1.38	hYVH1	61674.8	67400.3	67944.8	65831.9	40313.5	36540.6
VDEMKILPVLGSQTGKI	[5] Biotin K [16] Biotin K	2.18	hYVH1	50113.0	365513.8	357994.7	283363.4	136923.5	141605.2
VDEMKILPVLGSQTGKI	[4] Oxidation M [5] Biotin K [16] Biotin K	2.12	hYVH1	291418.8	240737.1	236726.2	152099.9	101603.5	108365.6
WITPAFQIHK	[10] Biotin K	2.39	hYVH1	10191.4	10615.6	10189.3	2042.8	5216.1	5698.8
YPELQNLQELFAVDPTTVSQGLKDEVLYKCR	[30] Biotin K [31] Carbamidomethyl C	4.37	hYVH1	0.0	7334.0	6549.7	450.6	1585.2	1138.1

**Figure 3.6 MS spectra of biotinylated peptides.** **A)** Representative mass spectra of NHS-biotin treated samples from HeLa cells transfected with His-Hsp70 and FLAG-hYVH1 (top) and transfected with FLAG-hYVH1 and Myc-Src (bottom). **B)** A bar graph displaying the significant biotinylated peptide corresponding to amino acids 50-77, relative to a control peptide that remained unchanged in abundance between samples. All biotin-containing peptides were considered for normalization to acquire a correction factor to apply using the Progenesis software. Peptides reproducibly above a 1.5-fold

change were considered significant. (n=3) **C)** Tables showing significant peptides identified from all three trials of the NHS-biotin labelling experiment. The peptide corresponding to amino acids 50-77 is highlighted in red, the control peptide selected is highlighted in blue.

For statistical processing, all identified peptides were included for normalization by the Progenesis software to total peptide abundance to account for differences in sample concentrations. For structural information, we focused on biotinylated peptides that reproducibly met the rigorous criteria and displayed greater than a 1.5-fold difference in biotinylation between hYVH1 and hYVH1-Hsp70 samples after normalization. This analysis yielded a differentially biotinylated peptide corresponding to amino acid position 50-77, that displayed a statistically significant 62% reduction in biotinylation when Hsp70 was co-transfected with hYVH1. Intriguingly, this peptide includes the 68-77 peptide that was initially identified through the limited proteolysis method. This reproducibility between methods lends credibility to using differential biotin labelling for binding site identification while simultaneously strengthening the argument that the N-terminal domain of hYVH1 possesses the surface required for binding Hsp70.

We can contextualize the result of the binding site experiments by examining the X-ray, three-dimensional structure of the hYVH1 N-terminus. From the structure, it is apparent that the 50-77 peptide region presents as a solvent-exposed loop consisting of several charged residues (**Figure 3.7A**). Considering that the interaction between hYVH1 and Hsp70 is regulated by Src, we hypothesize that the displacement of this loop may occur in response to a phosphate introduction and possible electrostatic repulsions with Asp74, Glu73, or electrostatic attraction to Lys67 (**Figure 3.7B**). Future attempts to

characterize this interaction should consider the impact of mutagenesis of these residues on the ability of hYVH1 to bind Hsp70.

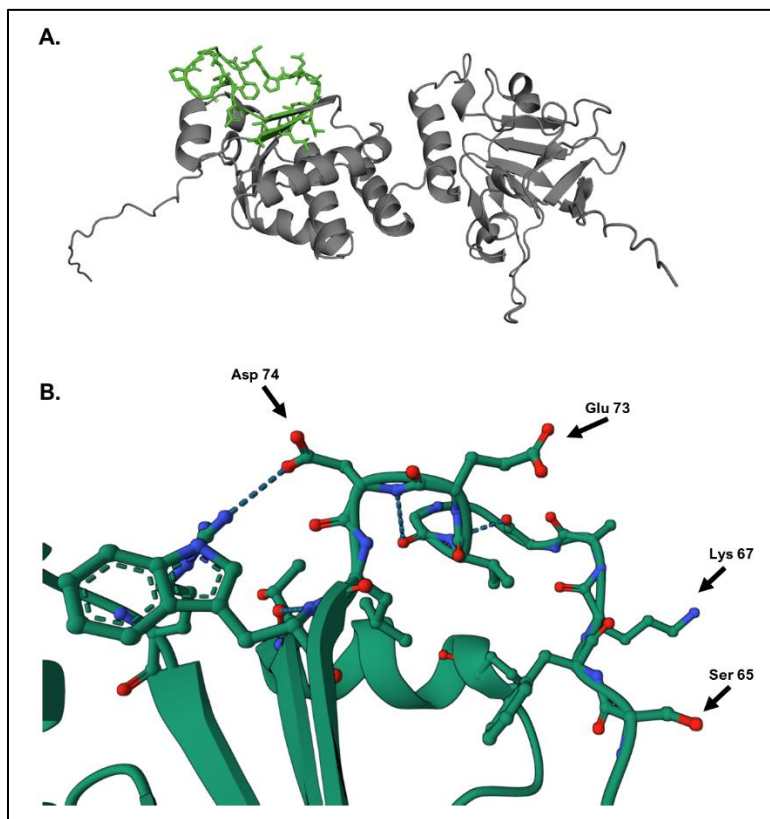


**Figure 3.7 The proposed N-terminal binding region on hYVH1.** A) The predicted structure of hYVH1 with the proposed Hsp70-binding region highlighted in green, with side chains visible. Structure produced in PyMOL. B) A zoomed-in view of the binding site structure, with Asp74, Glu73, Lys67, and Ser65 highlighted. Image produced from the hYVH1 N-terminal crystal structure on the Protein Data Bank (Accession: 4JNB).

#### 3.3.4 N-terminal coIP of hYVH1

With the finding from our structural mass spectrometry efforts that hYVH1 possesses a potential N-terminal binding surface for associating with Hsp70, we were interested in supporting this result using deletion constructs that were already available in the laboratory. An experiment was performed to replicate the originally unsuccessful coIP of Hsp70 with a ZBD-deleted mutant of hYVH1  $\Delta$ ZBD that featured only residues

1-173. The transfected samples included: empty vector (EV); Hsp70; Hsp70 and WT hYVH1; Hsp70 and hYVH1  $\Delta$ ZBD; Hsp70, hYVH1  $\Delta$ ZBD and Src; Hsp70 and Src; hYVH1  $\Delta$ ZBD and Src; and Src alone (**Figure 3.8**). All hYVH1 constructs were FLAG-tagged and the Hsp70 construct is His<sub>6</sub>-tagged.

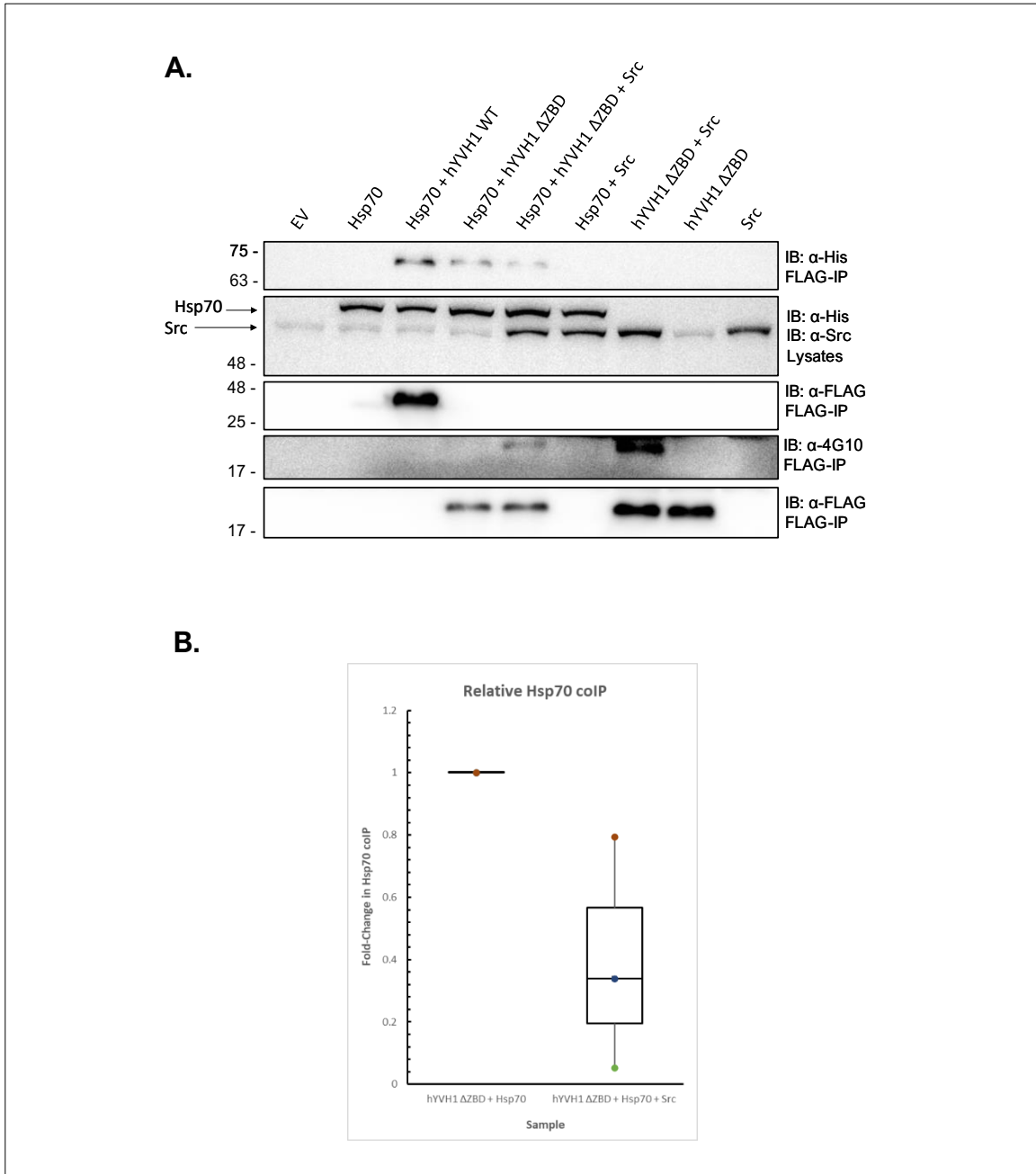


**Figure 3.8. N-terminal coIP of Hsp70 by hYVH1.** A) HeLa cells transfected with the indicated samples were lysed and subjected to a FLAG IP. From left to right: empty

vector (EV), Hsp70, Hsp70 + hYVH1 WT, Hsp70 + hYVH1  $\Delta$ ZBD, Hsp70 + hYVH1  $\Delta$ ZBD + Src, Hsp70 + Src, hYVH1  $\Delta$ ZBD + Src, hYVH1  $\Delta$ ZBD, and Src. The 5 panels shown are in descending mass order (kDa; shown on the left) and depict (from top to bottom): anti-His on a FLAG-IP, anti-His + anti-Src on lysates, anti-FLAG on a FLAG-IP, anti-4G10 on a FLAG-IP, and anti-FLAG on a FLAG-IP. hYVH1 is FLAG-tagged whereas Hsp70 is His<sub>6</sub>-tagged. **B**) ImageJ-obtained densitometry measurements of anti-His blots for the 4<sup>th</sup> and 5<sup>th</sup> lanes (sample ID on x-axis). Normalized to the amount of FLAG-hYVH1 present in the FLAG-IP and His-Hsp70 present in the lysates (n=3).

In this experiment (**Figure 3.8A**), the top panel illustrates the ability of each sample to coIP Hsp70. The His blot performed on FLAG-IPs (top panel) should not be expected to return a band for Hsp70 unless Hsp70 was co-enriched by a FLAG-tagged construct (hYVH1). Unexpectedly, the 4<sup>th</sup> and 5<sup>th</sup> lanes, both expressing hYVH1  $\Delta$ ZBD, were able to pull down diminished levels of Hsp70. It was determined through densitometry analysis (**Figure 3.8B**) that the sample in the 5<sup>th</sup> lane (expressing hYVH1  $\Delta$ ZBD, Hsp70 and Src) coprecipitated ~65% less Hsp70 on average than the sample without Src (4<sup>th</sup> lane), indicating that the ability of Src to separate the complex is maintained. However, the high variability across replicates rendered this finding not statistically significant although the trend was reproducible.

Most fascinating about this finding was that the N-terminal hYVH1 mutant used in this experiment lacked Tyr179 – the only identified Src phosphorylation site on hYVH1. Furthermore, both lanes that expressed hYVH1  $\Delta$ ZBD and Src (**Figure 3.8A** – 4<sup>th</sup> panel, lanes 5 and 7) demonstrated Tyr phosphorylation of the hYVH1 N-terminus through a 4G10 blot, signifying the presence of another Src-mediated pTyr site in addition to Tyr179. This prompted further exploration into the Src-mediated phosphorylation sites that were present on hYVH1 and their potential roles in driving the complex dissociation.

### 3.4 Phosphosite Mapping of hYVH1

#### 3.4.1 Validating the Presence of Alternative Sites

Though the N-terminal location of a phosphosite was novel information, the revelation of an alternative pTyr site on hYVH1 was a concept that had been explored previously. Past efforts to co-express hYVH1 Y179F with Src had shown that hYVH1 Y179F could still be phosphorylated on a Tyr residue, although attempts to locate that residue were unsuccessful. To illustrate this phosphorylation event, as well as confirm the presence of an alternative phosphorylation site, cells were transfected with either hYVH1 and empty vector or hYVH1 and Src in 2 replicates. All the samples were treated in culture with sodium orthovanadate to saturate phosphorylation sites, lysed, FLAG-immunoprecipitated, and one replicate was subjected to an alkaline phosphatase treatment to verify a removable phosphate via the anti-pTyr 4G10 blot (**Figure 3.9**).

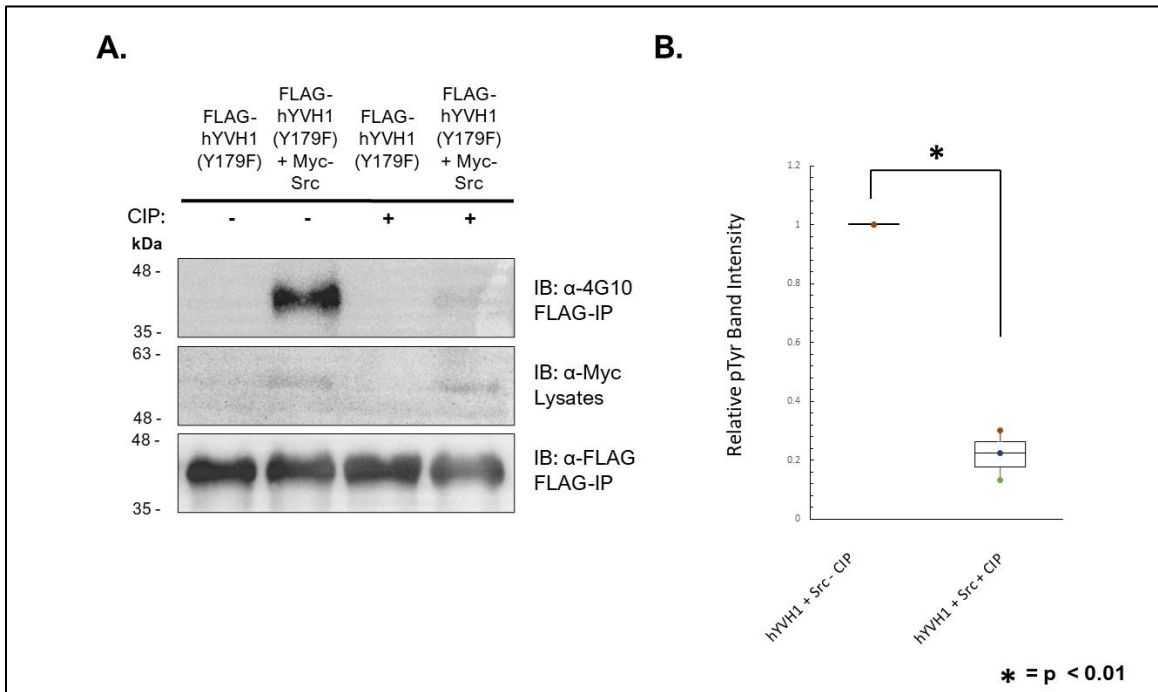


**Figure 3.9. Src Phosphorylation of hYVH1 Y179F.** A) A Western blot showing the phosphorylation of hYVH1 Y179F by Src following FLAG IP from HeLa cells. Samples are overexpressing FLAG-hYVH1 Y179F, or FLAG-hYVH1 Y179F and Myc-Src. The two lanes on the left have not been treated with alkaline phosphatase, and the two lanes on the right have. All four lanes have been treated with sodium orthovanadate. The top panel shows Tyr phosphorylation on a FLAG-IP, the middle panel shows the presence of Src in the cellular lysates, and the bottom panel verifies the amount of FLAG-hYVH1 in each lane. B) ImageJ-obtained densitometry measurements of 4G10 blots for the two Src-transfected lanes. Normalized to the amount of FLAG-hYVH1 and Myc-Src present in each sample (n=3).

This result (**Figure 3.9A**) shows that hYVH1 Y179F displays tyrosine phosphorylation when Src is co-expressed. Furthermore, the alkaline phosphatase treatment indicates that this signal can be reversed by ~78% to ensure that the signal on the 4G10 blot was not due to non-specific antibody binding. This immunoblot signifies that hYVH1 possesses an additional Src-mediated pTyr site that was not identified by mass spectrometry during the discovery of pTyr179, which was located through standard trypsin-directed proteolysis.<sup>60</sup> When considering why additional phosphorylation sites were previously missed, one issue is that some Tyr residues in the hYVH1 sequence (e.g. Tyr142 and Tyr182) reside in small, polar tryptic peptides (**Figure 3.10**).<sup>12</sup> This idea led to an assumption that these small, tryptic peptides may elute too readily from an RPLC column and be excluded from MS analysis.

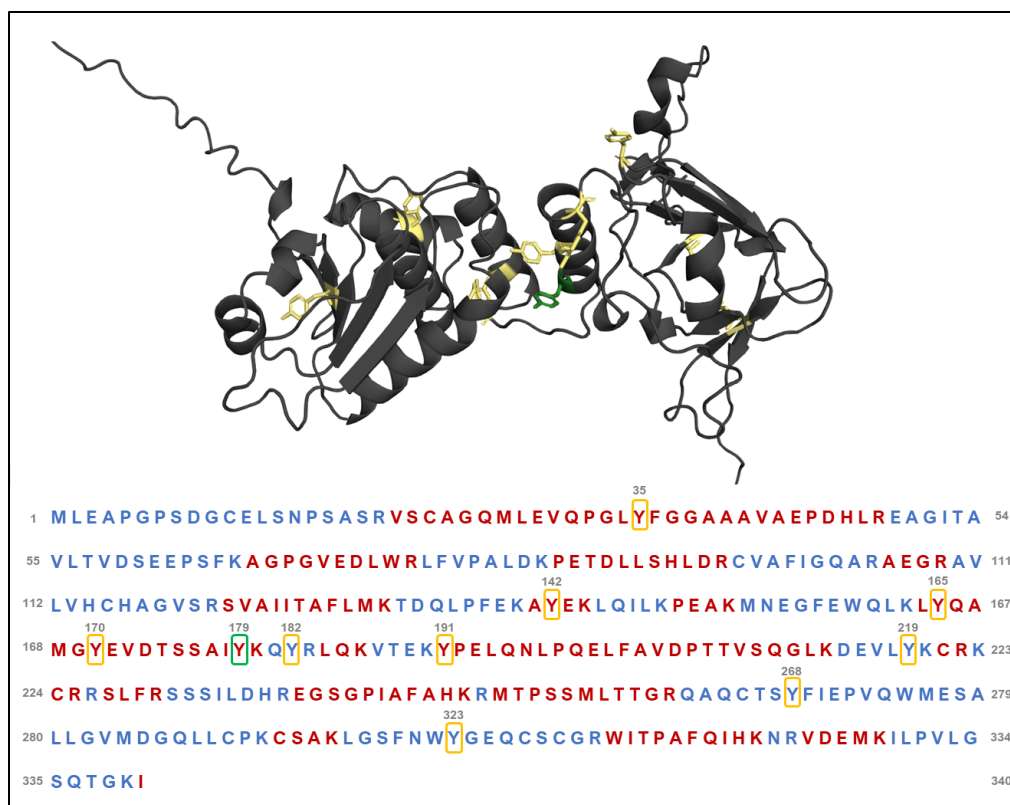


**Figure 3.10 Potential phosphotyrosine sites on hYVH1.** The 3D structure of hYVH1 with all Tyr residues in yellow, and Tyr179 in green. These are highlighted and numbered on the amino acid sequence below, which is coloured in alternating red and blue to delineate the boundaries of possible tryptic peptides (excluding the probable missed cleavages). Structure produced in PyMOL.

To address this concern, longer, alternative peptide fragments were obtained by repeating the original in-gel digestion protocol that found Tyr179, except with GluC or pepsin in place of trypsin (not shown). However, these results were largely inconclusive and failed to identify a novel pTyr site. Limited trypsin proteolysis was also attempted, where missed cleavages were induced to create larger peptides that would be more favourably retained. However, these experiments were also unsuccessful. To determine the identity of the unknown phosphorylation site, it was evident that a new instrumental approach needed to be developed.

### 3.4.2 SRM Mass Spectrometry with Ion Mobility

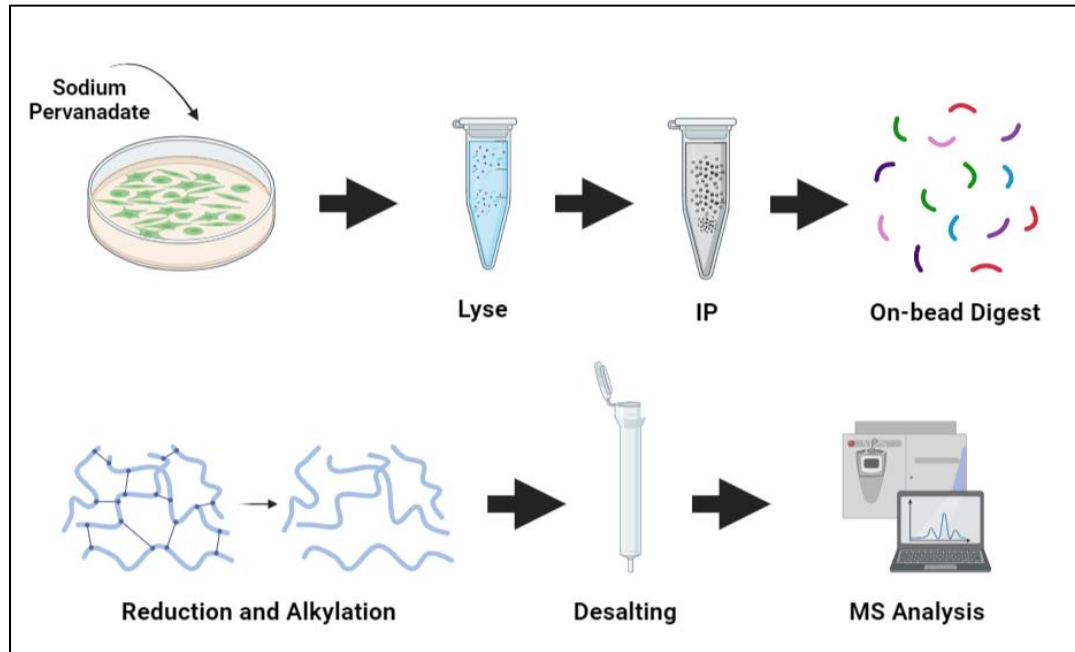


**Figure 3.11 Workflow for hYVH1 phosphosite mapping.** HeLa cells in culture were transfected with either hYVH1 + EV or hYVH1 + Src, then treated with sodium pervanadate for 1 hour before lysis. FLAG-IP was performed to isolate hYVH1, followed by an on-bead digestion with trypsin. Samples were then reduced and alkylated with DTT and IAA, before cleanup with an Oasis column and subsequent MS analysis. Figure produced in BioRender.

For more comprehensive phosphosite mapping, a novel approach was designed to improve the sequence coverage of in-solution trypsin proteolysis and increase the instrumental sensitivity for phosphorylated peptides (**Figure 3.11**). Similar to previous attempts, cells were transfected with hYVH1 and EV or hYVH1 and Src to evaluate the phosphorylation sites that are a consequence of Src co-expression. Sodium pervanadate was once again used to inhibit PTP activity to capture transient phosphorylation states. One notable optimization from the method that discovered pTyr179 was the inclusion of peptide reduction and alkylation, which was performed in the same manner as the NHS-biotin protocol.

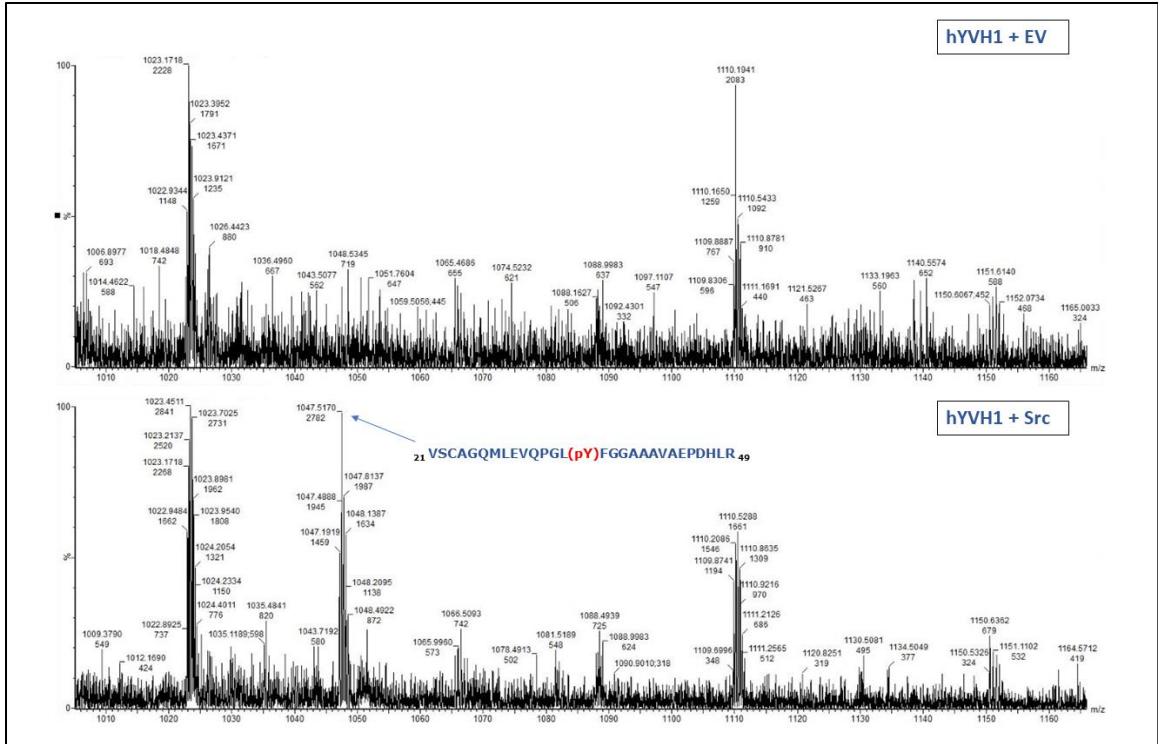


**Figure 3.12 MS fingerprint for phosphosite mapping.** An MS “fingerprint” spectrum that outlines the abundances of precursor peptide ions for both the hYVH1 + EV sample (top) and the hYVH1 + Src sample (bottom).

As shown in Figure 3.12, a peptide at an  $m/z$  of  $\sim 1047.5$  in the sample co-transfected with Src was observed that was absent in the sample without Src. This  $m/z$  value corresponds to a +3 peptide ion containing amino acid positions 21–49, and the additional mass of a phosphate moiety and a carbamidomethyl group. While carbamidomethyl modification is the consequence of the alkylation of Cys23, there are two possible residues on this peptide that may be phosphorylated: Ser22 and Tyr35. Initial attempts to sequence this peptide by DDA-mode MS/MS were unsuccessful due to its low abundance relative to the most abundant peptides in the spectrum.

To resolve this, a targeted-MS technique known as *selected-ion reaction monitoring* (SRM) was employed alongside the travelling wave ion mobility technology

(T-wave) of the SYNAPT G2-Si mass spectrometer. In this process, the instrument is programmed to isolate one precursor ion and synchronize the instrument to sample all of its fragment ions preferentially. The ion mobility functional mode can be used to further separate ions by shape, as more densely charged ions will travel further along it, and the ion “pusher” of the TOF can be set to delay ion sampling until the expected moment when the fragment ions are in position.<sup>76</sup> This method increases instrumental sensitivity to a particular peptide and enhances detection of fragment ions for comprehensive sequencing of targeted peptides.

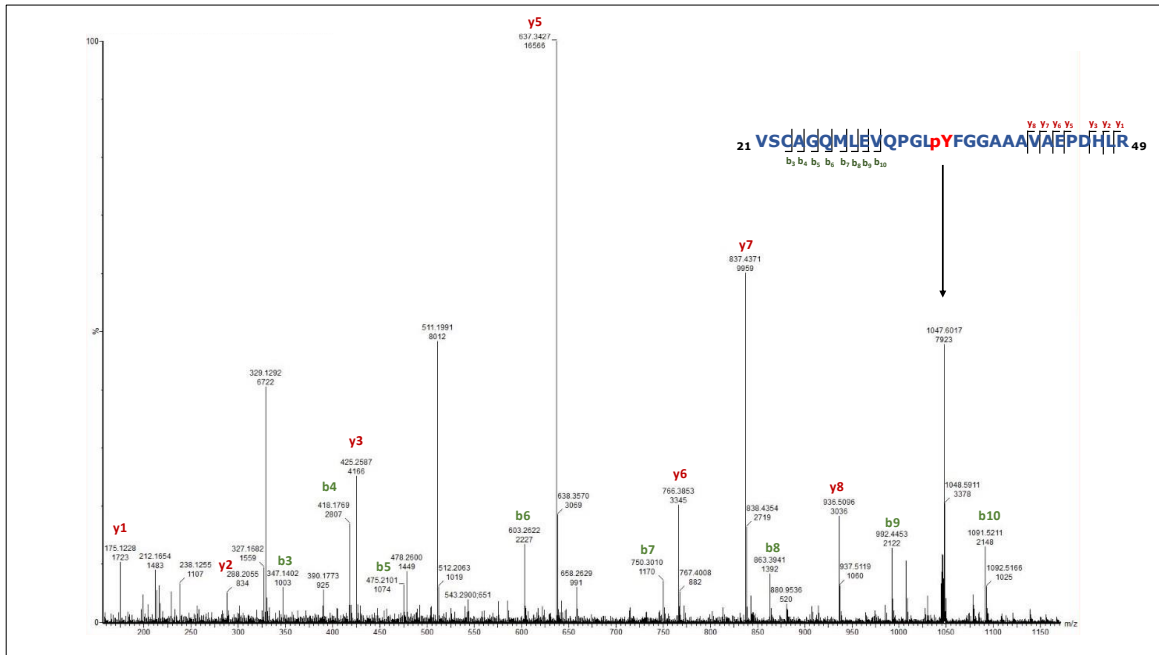


**Figure 3.13. MS/MS of a putative phosphorylation site.** An MS/MS spectrum produced from the fragmentation of the tryptic peptide located between amino acid positions 21-49, resolved using SRM techniques. The precursor ion is indicated by the arrow, with the sequence above showing the positions of the *y* and *b* ions. *y* and *b* ions are indicated on the spectrum above their respective peaks.

As can be seen from the abundance of detected *y* and *b* ions in the MS/MS spectrum (**Figure 3.13**), the sampling of the fragment ions from this peptide was greatly enhanced by SRM. Furthermore, the *b* ion series all correspond to the mass of unphosphorylated Ser, leaving the Tyr residue as the only possible phosphorylation target. The presence of the alkylated Cys23 suggests that the introduction of alkylation to the protocol is likely why this peptide is detectable now, as opposed to preceding efforts. This finding confirms that hYVH1 possesses a novel Src-mediated phosphorylation site on Tyr35.

#### *3.4.3 Characterization of Y35E Phosphorylation*

The identification of this new phosphorylation site invited further speculation into the dissociation mechanism of hYVH1 from Hsp70. Unlike Tyr179 – the previously identified Src phosphorylation site that is located in the linker region between domains – Tyr35 is present in the N-terminus, only ~30 residues upstream of the identified Hsp70 binding interface. The residue is solvent-exposed and proximal to a glutamic acid residue that it could potentially interact with (**Figure 3.14A**). Additionally, Tyr35 displayed evolutionary conservation with orthologues from both simple eukaryotes and higher order mammals (**Figure 3.14B**). Interestingly, the only other Tyr that was conserved among all four of the species shown here was Tyr179. This provided a compelling reason to postulate that perhaps it is the phosphorylation of Tyr35 that is responsible for breaking the interaction with Hsp70.



other to express Hsp70 relative to the hYVH1 present. The Y35E value was then expressed as a ratio, with the WT protein expressed as “1”.

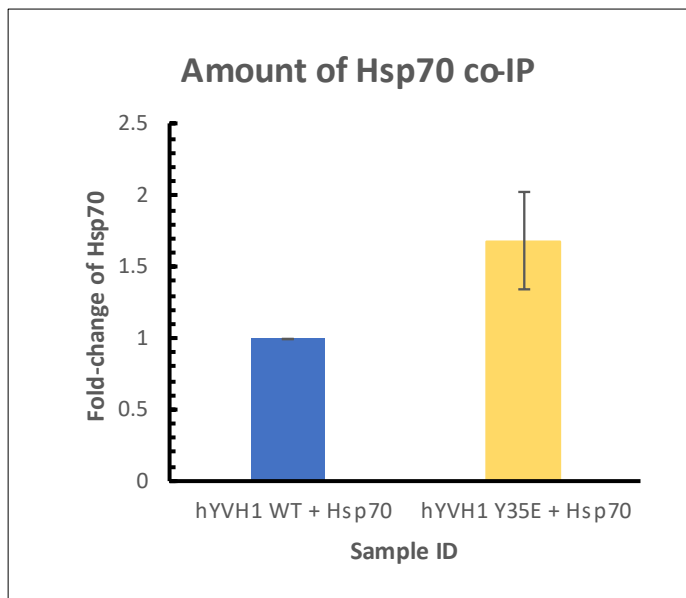


**Figure 3.15. MS results from hYVH1 Y35E and Hsp70 coIP.** A graph displaying the difference in Hsp70 coimmunoprecipitation between wild-type (WT) hYVH1 (blue) and hYVH1 Y35E (green) from HeLa cells. All hYVH1 and Hsp70 peptides were normalized to the top three most abundant peptides in each sample, and then normalized to the amount of hYVH1 between all trials and samples (n=3). All trials were then normalized to the WT sample, and the averages are expressed.

Unexpectedly, these results show an average increase of 68% in hYVH1-Hsp70 complex formation in response to the mutation of Tyr35 to a Glu (although the result was not statistically significant). This finding counterintuitively suggests that Src phosphorylation of hYVH1 at Tyr35 increases hYVH1-Hsp70 complex formation. The first consideration that must be made is the fidelity with which a glutamic acid residue emulates a phosphorylation site and the possibility that it may not be sufficiently sterically or electrostatically similar. Furthermore, the glutamic acid mutant provides a

constitutively phosphorylated state that may not be conducive to the protein's native state structure. This structural aberration may result in a misfolded protein that does not behave as hYVH1 normally would *in vivo*. We therefore cannot rule out that the Tyr35 mutation resulted in a variant that was misfolded. In that case, there is a possibility that the increase in Hsp70 pulldown may be a function of unfolded hYVH1 engaging with Hsp70 as a chaperone substrate through Hsp70's substrate-binding domain. This theory can be tested in future experiments by comparing the binding capability of hYVH1 Y35E to both domain-deleted mutants of Hsp70 (exclusively the ATPase domain and exclusively the substrate-binding domain). Phosphatase assays could also be performed in the future on both WT hYVH1 and hYVH1 Y35E, to assess if the mutant displays a decrease in enzymatic activity indicative of a compromised structure.

On the other hand, it is also possible that Y35E accurately mimics phosphorylated hYVH1, and that a toggling mechanism exists between high Hsp70 affinity and low Hsp70 affinity, depending on which residues are phosphorylated on hYVH1. There is a possibility that Tyr35 phosphorylation is a single event in a hierarchical pathway – where the ability to bind Hsp70 is dependent on the phosphorylation of Tyr35, but only if Tyr179 is phosphorylated. It may also be conceivable that the abrogation of hYVH1-Hsp70 binding is not a function of hYVH1 phosphorylation by Src but rather of Src phosphorylation on Hsp70. Others in the lab have produced results that indicate that Hsp70 is readily phosphorylated by Src when in complex with hYVH1.<sup>77</sup> Interestingly, under conditions of oxidative stress, the hYVH1-Hsp70 complex is unable to be attenuated by Src. Under these conditions, pTyr levels of Hsp70 decrease, while those of hYVH1 remain the same.<sup>77</sup> These results suggest it may be phosphorylation of Hsp70

that induces complex dissociation. It also suggests the possibility that pTyr35 may increase the hYVH1 affinity to Hsp70 to mediate the Src phosphorylation of Hsp70.

In conclusion, these results indicate that phosphorylation of Tyr35 may lead to an increase in the ability of hYVH1 to bind Hsp70. If the results produced are accurate, this may provide support for the hypothesis that hYVH1 plays a scaffolding role to recruit Src to phosphorylate Hsp70, of which one consequence is the disassembly of the hYVH1-Hsp70 complex.

### 3.5 Proposed Model

Compounding evidence from yeast models indicates that the mediation of late-stage, 60S ribosome biogenesis may be the primary function of hYVH1 in the cell, with other characteristics attributed to hYVH1 exhibiting functional interplay with this mechanism. Hsp70 performs a well-defined role at the ribosome in polypeptide synthesis by stabilizing and folding nascent polypeptide chains.<sup>54</sup> In addition, Ssa – an Hsp70 orthologue in yeasts – plays a role in yeast ribosome biogenesis as a release factor and exists in a temporally similar setting to that in which YVH1 is observed.<sup>62</sup> With hYVH1 and Hsp70 demonstrating a capability to associate with each other and colocalize under stress, there is a possibility that this interaction serves to attenuate ribosome biogenesis and redirect the complex to a cell survival function. This downregulation in ribosomal assembly would allow the cell to conserve the energy expenditure associated with translation while potentially forming stress granules to conserve translational machinery and withstand unfavourable conditions. If the cell survives, a growth factor-initiated cascade may signal the activation of Src kinase and the subsequent abrogation of the hYVH1-Hsp70 complex, liberating both proteins to allow hYVH1 to resume its role in ribosome biogenesis.

The Hsp70-hYVH1 complex may serve a functional purpose in cell survival when intact. Once critical interacting residues are identified on the binding regions of both hYVH1 and Hsp70, point mutants can be developed to evaluate the exact functions attributed to both complex presence and absence. One context where this might be valuable is at the stress granule, where the intact hYVH1-Hsp70 complex may be required to dissociate stress granules. For example, a dominant-negative mutant of

hYVH1 that cannot associate with Hsp70 would be valuable in determining if the complex is required to perform this function.

Integrating this information with our current working model, free hYVH1 may be preferentially phosphorylated by Src at Tyr35 under stress conditions. This phosphoisoform may possess increased binding affinity for Hsp70, which results in increased complex formation at the ribosome under stress conditions, or at the stress granule in stress recovery. When hYVH1 is complexed, this phosphorylation event may also be responsible for the recruitment of Src to the Hsp70-hYVH1 complex, where it then eventually phosphorylates Hsp70 to release the interaction. This would then return hYVH1 and Hsp70 to their regular cellular functions. While providing a compelling narrative, there needs to be further investigation into this mechanism through *in vitro* methods, localization experiments, and more thorough mutation studies before conclusions like this can be drawn. In the meantime, the speculation provided here will serve to inform future inquiry into the phospho-dependency of hYVH1's interactions.

## CHAPTER 4: CONCLUSION AND FUTURE WORK

### 4.1 Conclusions

Through the efforts discussed herein, evidence was provided to indicate that Src phosphorylation of hYVH1 is reproducible at endogenous expression levels, providing a basal physiological context for the interactions witnessed in overexpressed cellular models and *in vitro* experiments. Results obtained from MS-based limited proteolysis and biotinylation approaches support previous findings of the Hsp70 binding site existing on the N-terminus of hYVH1. Specifically, spectra point to a general peptide region between amino acids 50-77, suggesting that the devised biotin labelling method may be analogous to limited proteolysis methods for this application. Also detailed here was the discovery of a novel Src-mediated phosphorylation site on the conserved Tyr35 residue in the catalytic domain of hYVH1. This residue lies just upstream of the putative Hsp70 binding site. Phosphomimetic mutant studies provide preliminary evidence that the association between these two proteins may be modulated by the phosphorylation of Tyr35, which, when phosphorylated, may lead to an increase in the hYVH1-Hsp70 association. This disparity in the phosphoisoforms that can bind Hsp70 may imply the existence of factors on Hsp70 responsible for mediating the complex disassociation. It is hypothesized that the phosphorylation of Tyr35 may be a singular step in a hierarchical phosphorylation system that recruits Hsp70 for complex formation and subsequent cytoprotective action. This complex may be relevant in undefined roles in stress granule disassembly or ribosome biogenesis.

In summary, this research provides arguments for a mechanism by which hYVH1 and Hsp70 may interact in a phospho-dependent manner, as shown through mass spectrometric techniques. It also showcases the discovery of a novel Src phosphorylation site on hYVH1 that may alter the binding capacity of these two proteins.

## 4.2 Future Work

Although the endogenous phosphorylation of hYVH1 has been demonstrated, attempts to provide better resolution on more physiologically consistent cellular models should be undertaken. This work may also be translated to more disease-relevant models that have been known to highly express hYVH1 (i.e., CML, ependymomas) and oncogenic Src. Regarding the binding interface, more insight must be given into the structural elements on Hsp70 that are amenable to binding hYVH1, including mapping Src-mediated phosphorylation sites on Hsp70. This likely would involve a similar technique to the one demonstrated here, complete with pervanadate stimulation, SRM-MS and phosphopeptide enrichment columns that may be necessary to bring pTyr levels to a detectable threshold.

For more accurate characterization of the binding interface, a mass spectrometric approach with higher resolution could be utilized, such as cross-linking MS, to provide detail for specific residues that are in proximity and potentially responsible for this interaction on both proteins. It may also be advantageous to study this interaction by using purified hYVH1, Hsp70 and Src *in vitro* to observe if the complex is sustained outside of a cellular environment. Furthermore, once critical interacting residues on hYVH1 are identified, mutants that are devoid of these specific residues may be

generated and overexpressed in *hyvh1*-silenced models. These complex-deficient cells can then be assessed for their ability to disassemble stress granules, or for their translation efficiency in response to stress recovery, to characterize the intracellular purpose of hYVH1-Hsp70 association.

To pursue the interrogation of Tyr35 function through mutation studies, the following mutants of hYVH1 can provide a more comprehensive inquiry into the role of Tyr35 phosphorylation: Y35F, Y179F & Y35F (double mutant), and Y179E & Y35E (double mutant). These mutants may also be transfected with Src and Hsp70 to assess the changes in their ability to coIP Hsp70 in response to Src phosphorylation. Furthermore, while this research focuses on Src-mediated tyrosine phosphorylation as a potential mediator of this complex, there is still a possibility that Ser/Thr phosphorylation may play a role as well, and it may be advantageous to map and assess these phosphorylation sites for a more holistic representation of the complex. A recommended starting point would be mutation of Ser14 and Ser335 on hYVH1, which were both previously implicated in the cell cycle regulation functions of hYVH1.

## REFERENCES

1. Muda, M., Manning, E. R., Orth, K. & Dixon, J. E. Identification of the Human YVH1 Protein-tyrosine Phosphatase Orthologue Reveals a Novel Zinc Binding Domain Essential for in Vivo Function. *J Biol Chem* **274**, 23991-23995. <http://www.jbc.org/> (1999).
2. Pino, L. K., Rose, J., O'Broin, A., Shah, S. & Schilling, B. Emerging mass spectrometry-based proteomics methodologies for novel biomedical applications. *Biochemical Society Transactions* **48**, 1953–1966 Preprint at <https://doi.org/10.1042/BST20191091> (2020).
3. Cui, M., Cheng, C. & Zhang, L. High-throughput proteomics: a methodological mini-review. *Laboratory Investigation* **102**, 1170–1181 Preprint at <https://doi.org/10.1038/s41374-022-00830-7> (2022).
4. Walther, T. C. & Mann, M. Mass spectrometry-based proteomics in cell biology. *Journal of Cell Biology* **190**, 491–500 Preprint at <https://doi.org/10.1083/jcb.201004052> (2010).
5. Watson, J. Throck. & Sparkman, O. D. Introduction to mass spectrometry: instrumentation, applications and strategies for data interpretation. (John Wiley & Sons, 2007).
6. Zhang, Y., Fonslow, B. R., Shan, B., Baek, M. C. & Yates, J. R. Protein analysis by shotgun/bottom-up proteomics. *Chemical Reviews* **113**, 2343–2394 Preprint at <https://doi.org/10.1021/cr3003533> (2013).
7. Zhang, G. *et al.* Protein quantitation using mass spectrometry. *Methods Mol Biol* **673**, 211–222 (2010).
8. Richards, A. L., Eckhardt, M. & Krogan, N. J. Mass spectrometry-based protein–protein interaction networks for the study of human diseases. *Mol Syst Biol* **17** (2021).
9. Artigues, A. *et al.* Protein structural analysis via mass spectrometry-based proteomics. *Adv Exp Med Biol* **919** 397–431 (2016).
10. Westphall, M. S. *et al.* Three-dimensional structure determination of protein complexes using matrix-landing mass spectrometry. *Nat Commun* **13** (2022).
11. Doll, S. & Burlingame, A. L. Mass spectrometry-based detection and assignment of protein posttranslational modifications. *ACS Chemical Biology* **10**, 63–71 Preprint at <https://doi.org/10.1021/cb500904b> (2015).
12. Dephoure, N., Gould, K. L., Gygi, S. P. & Kellogg, D. R. Mapping and analysis of phosphorylation sites: A quick guide for cell biologists. *Mol Biol Cell*. **24**, 535–542 Preprint at <https://doi.org/10.1091/mbc.E12-09-0677> (2013).

13. Karas, M., Bachmann, D., Bahr, U. & Hillenkamp, F. Matrix-assisted ultraviolet laser desorption of non-volatile compounds. *Int J Mass Spectrom Ion Process* **78**, 53–68 (1987).
14. Fenn, J. B., Mann, M., Meng, C. K., Wong, S. F. & Whitehouse, C. M. Electrospray Ionization for Mass Spectrometry of Large Biomolecules. *Science (1979)* **246**, 64–71 (1989).
15. Bian, Y. *et al.* Robust, reproducible and quantitative analysis of thousands of proteomes by micro-flow LC–MS/MS. *Nat Commun.* **11** (2020).
16. Allen, D. R. & Mcwhinney, B. C. Quadrupole Time-of-Flight Mass Spectrometry: A Paradigm Shift in Toxicology Screening Applications. *Clin Biochem Rev* **40**, 135–146 (2019).
17. Su, T. *et al.* A comparative study of data-dependent acquisition and data-independent acquisition in proteomics analysis of clinical lung cancer tissues constrained by blood contamination. *Proteomics Clin Appl* **16** (2022). doi: 10.1002/prca.202000099.
18. Voet, D., Voet, J. G. & Pratt, C. W. Fundamentals of Biochemistry (5th edition) Life at the Molecular Level. (John Wiley and Sons, 2016).
19. Murn, J. & Shi, Y. The winding path of protein methylation research: Milestones and new frontiers. *Nat Rev Mol Cell Biol.* **18**, 517–527 Preprint at <https://doi.org/10.1038/nrm.2017.35> (2017).
20. Drazic, A., Myklebust, L. M., Ree, R. & Arnesen, T. The world of protein acetylation. *Biochim Biophys Acta.* **1864**, 1372–1401 (2016).
21. Goth, C. K., Petä Jä -Repo, U. E. & Rosenkilde, M. M. G Protein-Coupled Receptors in the Sweet Spot: Glycosylation and other Post-translational Modifications. *ACS Pharmacol Transl Sci.* **3**, 237–245 (2020) doi:10.1021/acsptsci.0c00016.
22. Swatek, K. N. & Komander, D. Ubiquitin modifications. *Cell Research.* **26**, 399–422 (2016).
23. Khoury, G. A., Baliban, R. C. & Floudas, C. A. Proteome-wide post-translational modification statistics: frequency analysis and curation of the swiss-prot database. *Scientific reports.* **1**. (2011). doi:10.1038/srep00090.
24. Olsen, J. V *et al.* Global, In Vivo, and Site-Specific Phosphorylation Dynamics in Signaling Networks. *Cell.* **3**, 635–648 (2006). doi:10.1016/j.cell.2006.09.026.
25. Tautz, L., Critton, D. A. & Grotegut, S. Protein tyrosine phosphatases: Structure, function, and implication in human disease. *Methods in Molecular Biology* **1053**, 179–221 (2013).
26. Day, E. K., Sosale, N. G., Lazzara, M. J. Cell Signaling Regulation by Protein Phosphorylation: A Multivariate, Heterogeneous, and Context-dependent Process. *Curr Opin Biotechnol* **40**, 185–192 (2016).

27. Nardoizzi, J. D., Lott, K. & Cingolani, G. Phosphorylation meets nuclear import: a review. *Cell Commun Signal* **8**, 32 (2010).
28. Marjan Varedi, S. K., Ventura, A. C., Merajver, S. D., Nina Lin, X. & Di Bernardo, D. Multisite Phosphorylation Provides an Effective and Flexible Mechanism for Switch-Like Protein Degradation. *PLoS One* **5**, 14029 (2010).
29. Johnson, L. N., Barford, D. & Keck, W. M. The effects of phosphorylation on the structure and function of proteins. *Annu Rev Biophys Biomol Struct* **22**, 199-232 (1993).
30. Keniry, M. & Parsons, R. The role of PTEN signaling perturbations in cancer and in targeted therapy. *Oncogene* **27**, 5477–5485 (2008).
31. Cohen, P. The role of protein phosphorylation in human health and disease. The Sir Hans Krebs Medal Lecture. *Eur J Biochem* **268**, 5001–5010 (2001).
32. Krebs, E. G. & Fischer, E. H. Phosphorylase activity of skeletal muscle extracts. *J Biol Chem* **216**, 113–120 (1955).
33. Kresge, N., Simoni, R. D. & Hill, R. L. The Process of Reversible Phosphorylation: the Work of Edmond H. Fischer. *J Biol Chem* **286** (2011).
34. Alonso, A. *et al.* Protein Tyrosine Phosphatases in the Human Genome. *Cell* **117**(6):699-711 (2004).
35. Shi, Y. Serine/Threonine Phosphatases: Mechanism through Structure. *Cell* **139** 468–484 Preprint at <https://doi.org/10.1016/j.cell.2009.10.006> (2009).
36. Vaneynde, P., Verbinnen, I. & Janssens, V. The role of serine/threonine phosphatases in human development: Evidence from congenital disorders. *Frontiers in Cell and Developmental Biology*, **10**. Preprint at <https://doi.org/10.3389/fcell.2022.1030119> (2022).
37. Liu, K. E., Lemon, B. & Traktman, P. The Dual-Specificity Phosphatase Encoded by Vaccinia Virus, VH1, Is Essential for Viral Transcription In Vivo and In Vitro. *Journal of virology*, **69** (1995).
38. Guan, K. *et al.* A yeast protein phosphatase related to the vaccinia virus VH1 phosphatase is induced by nitrogen starvation. *Proc Natl Acad Sci USA*. **89**, 12175-12179. (1992).
39. Sun, H., Charles, C. H., Lau, L. F. & Tonks, N. K. MKP-1 (3CH134), an Immediate Early Gene Product, Is a Dual Specificity Phosphatase That Dephosphorylates MAP Kinase In Vivo. *Cell*, **75** (1993).
40. Mendrzyk, F. *et al.* Identification of gains on 1q and epidermal growth factor receptor overexpression as independent prognostic markers in intracranial ependymoma. *Clinical Cancer Research* **12**, 2070–2079 (2006).

41. Gratiias, S. *et al.* Genomic gains on chromosome 1q in retinoblastoma: Consequences on gene expression and association with clinical manifestation. *Int J Cancer* **116**, 555–563 (2005).
42. Hirai, M. *et al.* q23 Gain Is Associated With Progressive Neuroblastoma Resistant to Aggressive Treatment. *Genes Chromosomes Cancer* **25**, 261–269 (1999).
43. Sharda, P. R., Bonham, C. A., Mucaki, E. J., Butt, Z. & Vacratsis, P. O. The dual-specificity phosphatase hYVH1 interacts with Hsp70 and prevents heat-shock-induced cell death. *Biochemical Journal* **418**, 391–401 (2009).
44. Pavic, K., Duan, G. & Köhn, M. VHR/DUSP3 phosphatase: Structure, function and regulation. *FEBS Journal* **282**, 1871–1890 (2015).
45. Bonham, C. A. & Vacratsis, P. O. Redox regulation of the human dual specificity phosphatase YVH1 through disulfide bond formation. *Journal of Biological Chemistry* **284**, 22853–22854 (2009).
46. Kozarova, A., Hudson, J. W. & Vacratsis, P. O. The dual-specificity phosphatase hYVH1 (DUSP12) is a novel modulator of cellular DNA content. *Cell Cycle* **10**, 1669–1678 (2011).
47. Geng, Q., Xhabija, B., Knuckle, C., Bonham, C. A. & Vacratsis, P. O. The Atypical Dual Specificity Phosphatase hYVH1 Associates with Multiple Ribonucleoprotein Particles. *Journal of Biological Chemistry* **292**, 539–550 (2017).
48. Waterhouse, A. *et al.* SWISS-MODEL: Homology modelling of protein structures and complexes. *Nucleic Acids Res* **46**, 296–303 (2018).
49. Schrödinger, L. & DeLano, W. PyMOL. Preprint at (2020).
50. MacKeigan, J. P., Murphy, L. O. & Blenis, J. Sensitized RNAi screen of human kinases and phosphatases identifies new regulators of apoptosis and chemoresistance. *Nat Cell Biol* **7**, 591–600 (2005).
51. DaDalt, A. A., Bonham, C. A., Lotze, G. P., Luiso, A. A. & Vacratsis, P. O. Src-mediated phosphorylation of the ribosome biogenesis factor hYVH1 affects its localization, promoting partitioning to the 60S ribosomal subunit. *J Biol Chem* **298** (2022).
52. Buchan, J. R. & Parker, R. Eukaryotic Stress Granules: The Ins and Outs of Translation. *Mol Cell* **36**, 932–941 (2009).
53. Fritzsche, R. *et al.* Interactome of two diverse RNA granules links mRNA localization to translational repression in neurons. *Cell Rep* **5**, 1749–1762 (2013).
54. Mayer, M. P. & Bukau, B. Hsp70 chaperones: Cellular functions and molecular mechanism. *Cellular and Molecular Life Sciences* **62** 670–684 Preprint at <https://doi.org/10.1007/s00018-004-4464-6> (2005).

55. Velasco, L., Dublang, L., Moro, F. & Muga, A. The complex phosphorylation patterns that regulate the activity of Hsp70 and its cochaperones. *International Journal of Molecular Sciences* **20** Preprint at <https://doi.org/10.3390/ijms20174122> (2019).
56. Calderwood, S. K., Khaleque, M. A., Sawyer, D. B. & Ciocca, D. R. Heat shock proteins in cancer: Chaperones of tumorigenesis. *Trends in Biochemical Sciences* **31**, 164–172 Preprint at <https://doi.org/10.1016/j.tibs.2006.01.006> (2006).
57. Takayama, S., Xie, Z. & Reed, J. C. An evolutionarily conserved family of Hsp70/Hsc70 molecular chaperone regulators. *Journal of Biological Chemistry* **274**, 781–786 (1999).
58. Thomas, S. M. & Brugge, J. S. Cellular functions regulated by src family kinases. *Annu. Rev. Cell Dev. Biol* **13** (1997).
59. Roskoski, R. Src protein-tyrosine kinase structure, mechanism, and small molecule inhibitors. *Pharmacological Research* **94** 9–25. <https://doi.org/10.1016/j.phrs.2015.01.003> (2015).
60. DaDalt, A. A. Regulation of the Ribosome Biogenesis Factor hYVH1 by Src-mediated Phosphorylation. (University of Windsor, 2021).
61. Kemmler, S., Occhipinti, L., Veisu, M. & Panse, V. G. Yvh1 is required for a late maturation step in the 60S biogenesis pathway. *Journal of Cell Biology* **186**, 863–880 (2009).
62. Greber, B. J. Mechanistic insight into eukaryotic 60S ribosomal subunit biogenesis by cryo-electron microscopy. *RNA*, **22**, 1643–1662. <http://www.rnajournal.org/cgi/doi/10.1093/rna/naw001> (2016).
63. Gonzalez, R. L. Survivor: Ribosome Edition. *EMBO J*, **36**, 1996–1998 (2017).
64. Zhao, T. *et al.* Disome-seq reveals widespread ribosome collisions that promote cotranslational protein folding. *Genome Biol* **22** (2021).
65. Miluzio, A., Beugnet, A., Volta, V. & Biffo, S. Eukaryotic initiation factor 6 mediates a continuum between 60S ribosome biogenesis and translation. *EMBO Rep* **10**, 459–465 (2009).
66. Curcio, M. F. *et al.* Regulatory effects of nitric oxide on src kinase, FAK, p130Cas, and receptor protein tyrosine phosphatase alpha (PTP- $\alpha$ ): A Role for the cellular redox environment. *Antioxid Redox Signal* **13**, 109–125 (2010).
67. Irving, E. & Stoker, A. W. Vanadium compounds as PTP inhibitors. *Molecules*, **22** Preprint at <https://doi.org/10.3390/molecules22122269> (2017).
68. Huyer, G. *et al.* Mechanism of inhibition of protein-tyrosine phosphatases by vanadate and pervanadate. *Journal of Biological Chemistry* **272**, 843–851 (1997).

69. Weernink, P. A. O. & Rijksen, G. Activation and translocation of c-Src to the cytoskeleton by both platelet-derived growth factor and epidermal growth factor. *Journal of Biological Chemistry* **270**, 2264–2267 (1995).
70. Fiordalisi, J. J., Dewar, B. J., Graves, L. M., Madigan, J. P. & Cox, A. D. Src-Mediated Phosphorylation of the Tyrosine Phosphatase PRL-3 Is Required for PRL-3 Promotion of Rho Activation, Motility and Invasion. *PLoS One* **8** (2013).
71. Tian, G., Cory, M., Smith, A. A. & Blaine Knight, W. Structural determinants for potent, selective dual site inhibition of human pp60c-src by 4-anilinoquinazolines. *Biochemistry* **40**, 7084–7091 (2001).
72. Giannoni, E., Buricchi, F., Raugei, G., Ramponi, G. & Chiarugi, P. Intracellular Reactive Oxygen Species Activate Src Tyrosine Kinase during Cell Adhesion and Anchorage-Dependent Cell Growth. *Mol Cell Biol* **25**, 6391 (2005).
73. Roskoski, R. Src kinase regulation by phosphorylation and dephosphorylation. *Biochem Biophys Res Commun* **331**, 1–14 (2005).
74. Schopper, S. *et al.* Measuring protein structural changes on a proteome-wide scale using limited proteolysis-coupled mass spectrometry. *Nat Protoc* **12**, 2391–2410 (2017).
75. Wu, Z. *et al.* Domain structure and DNA binding regions of  $\beta$  protein from bacteriophage  $\lambda$ . *Journal of Biological Chemistry* **281**, 25205–25214 (2006).
76. Rojas Echeverri, J. C., Volke, D., Milkovska-Stamenova, S. & Hoffmann, R. Evaluating Peptide Fragment Ion Detection Using Traveling Wave Ion Mobility Spectrometry with Signal-Enhanced MSE(SEMSE). *Anal Chem* **94**, 10930–10941 (2022).
77. Lotze, G. P. Exploring the Impact of Src-Directed Phosphorylation on hYVH1's Intracellular Function. (University of Windsor, 2023).

# APPENDICES

## Appendix A

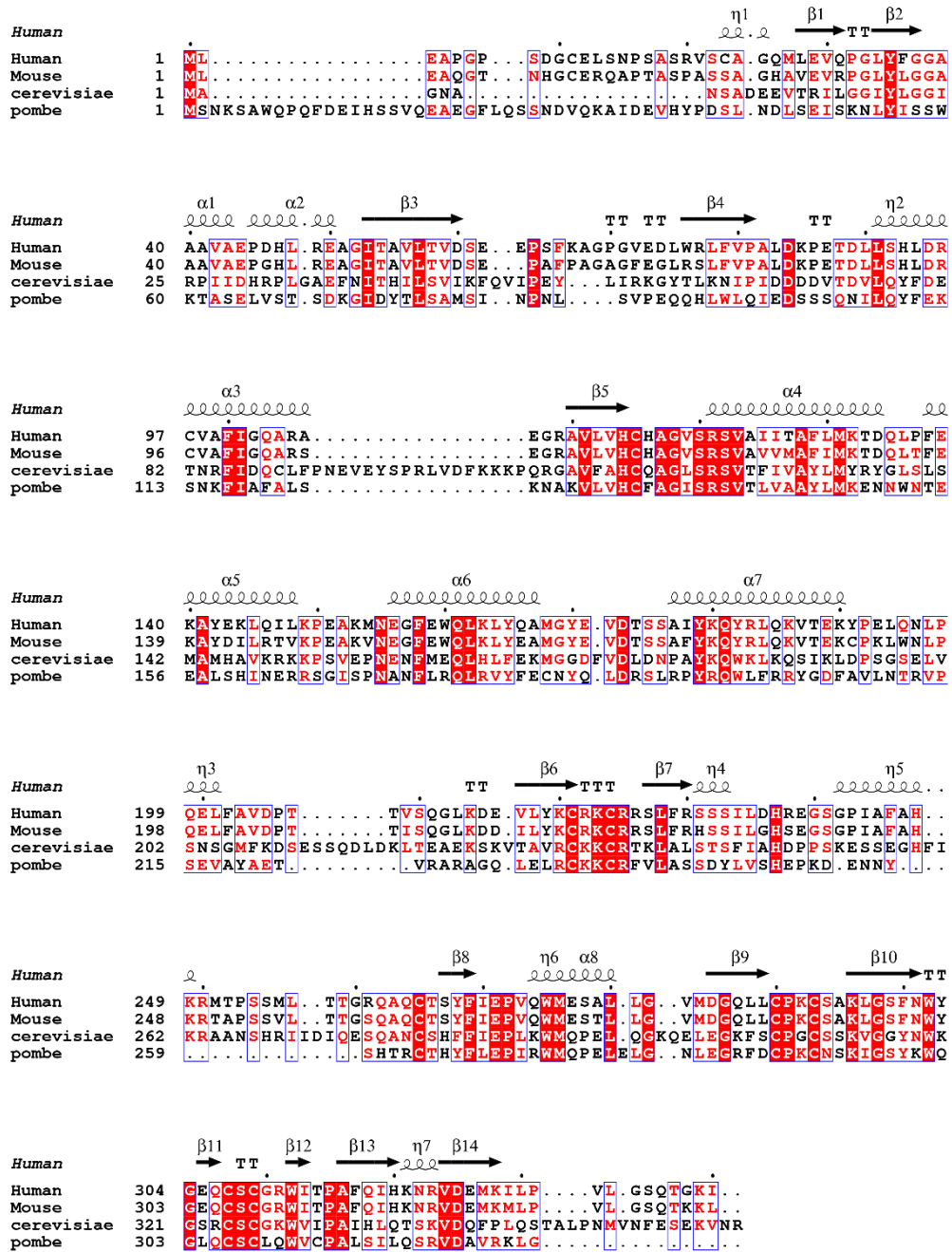


**Figure C.3.4. Full sequence alignment for hYVH1.** Sequence alignment for hYVH1 with the mouse MVH1 orthologue, and YVH1 orthologues from *S. cerevisiae* and *S. pombe*. The secondary structure of hYVH1 is shown above, and universally conserved residues are highlighted in red. Produced in ESPript.

## VITA AUCTORIS

NAME: Adrian Luiso

PLACE OF BIRTH: Windsor, ON

YEAR OF BIRTH: 1998

EDUCATION: Sandwich Secondary School, LaSalle, ON,  
2016

University of Windsor, B.Sc., Windsor, ON,  
2020